Copy
RM E52G02

NACA RM E52G02

RESEARCH MEMORANDUM

EFFECTS ON THE WEIGHT-FLOW RANGE AND EFFICIENCY OF A TYPICAL AXIAL-FLOW COMPRESSOR INLET STAGE THAT RESULT FROM THE USE OF A DECREASED BLADE CAMBER OR DECREASED GUIDE-VANE TURNING

By Robert J. Jackson

Lewis Flight Propulsion Laboratory
Cleveland, Ohio

NATIONAL ADVISORY COMMITTEE
FOR AERONAUTICS

WASHINGTON
September 19, 1952

NATIONAL ADVISORY COMMITTEE FOR AERONAUTICS

RESEARCH MEMORANDUM

EFFECTS ON THE WEIGHT-FLOW RANGE AND EFFICIENCY OF A TYPICAL AXIAL-FLOW COMPRESSOR INLET STAGE THAT RESULT FROM THE USE OF DECREASED BLADE CAMBER OR DECREASED GUIDE-VANE TURNING

By Robert J. Jackson

SUMMARY

An attempt to improve the part-speed weight-flow-range characteristics of a typical inlet stage was made by each of the following approaches: (a) increasing the usable range of angle of attack by a reduction in camber and (b) reducing the rate of change of angle of attack with weight flow by the use of decreased guide-vane turning. The following results were obtained:

The narrow usable weight-flow range exhibited by inlet-stage compressor designs, which feature high guide-vane turning in order to combine a subsonic Mach number limit with high wheel speed, was caused mainly by two factors: (a) high absolute inlet-air angles resulted in a rapid rate of change of angle of attack with axial velocity and (b) the comparatively low relative inlet velocities and the large static-pressure gradient downstream of the rotor resulted in an excessive pressure rise at the rotor-tip region and in a radial shift of flow towards the hub. The high pressure rise and radial flow may cause an excessive local pressure gradient on the blade surface. Both effects are most severe at the tip region where the additional effects of tip clearance and casing boundary layer may help lead to a premature flow separation. Hence, the over-all range is limited by the three-dimensional stall characteristics of this portion of the blade.

Decreased blade camber had very little effect on weight-flow range because it affected the pressure-rise characteristics and radial shift in flow only slightly. A large reduction in camber, hence in total-pressure ratio, would be required in order to realize any appreciable reduction in the static-pressure rise where the inlet conditions are the result of high guide-vane turning.

Reduction in the magnitude of guide-vane turning results in a large decrease in the rate of change of angle of attack with axial velocity.

Furthermore, for the rotor-configuration investigated, zero guide-vane turning established a downstream static-pressure gradient that required a less severe rate of pressure rise at the rotor tip and the flow did not shift in a radial direction. The results of this low pressure rise at the tip and approximately two-dimensional flow were high peak blade-element efficiency (reflected in high over-all efficiency) and increased usable range of angle of attack.

INTRODUCTION

Turbojet-engine performance requirements include high thrust and low specific fuel consumption. These factors establish the following specifications for design-speed compressor performance for present day applications: (a) high weight flow and (b) high over-all efficiency. These specifications should be approached as closely as possible over a wide range of speeds. In addition, good efficiencies at all speeds on the engine operating line are desirable for rapid acceleration characteristics. The investigation reported herein was conducted at the NACA Lewis laboratory to improve compressor part-speed performance.

Studies of off-design performance of multistage axial-flow compressors (reference 1) have indicated that these part-speed characteristics require that the inlet stage operate efficiently over a wide weight-flow range. The requirements for design-speed operation of the inlet stage include high tip speed (to permit high pressure ratios for the following stages), high weight flow per unit frontal area, and high stage-pressure ratio (to minimize engine size and weight). The inlet-stage-design problem, then, becomes one of obtaining the best compromise of the desired design-speed characteristics of high tip speed, weight flow, and stage-pressure ratio with wide weight-flow range at low speeds.

The weight-flow range over which the rotor of an inlet stage will operate with good efficiency depends upon (a) the rate of change of angle of attack with axial velocity at each of the radial blade elements, and (b) upon the efficient range of angle of attack for each blade section. The rate of change of angle of attack with axial velocity is a function of the velocity-diagram geometry; while the efficient range of angle of attack of a blade section in two-dimensional flow (reference 2) is a function of the blade camber, blade shape, solidity, and the relative inlet-air angle.

An attempt to improve the part-speed weight-flow-range characteristics of a typical inlet stage was made by (a) increasing the efficient range of angle of attack of the blade sections by a reduction in camber, and (b) reducing the rate of change of angle of attack by velocity-diagram changes.

[redacted]

The investigation was based on data from two inlet-type (0.5 hub-tip ratio) compressor rotors designed for the same inlet-velocity distribution and Mach number limit (about 0.7 at the design tip speed of 1104 ft/sec). Both rotors made use of NACA 65-series variable camber compressor blading. For the high-camber rotor, the theoretical free-stream lift coefficient varied from 1.69 at the hub to 0.87 at the tip; for the low-camber rotor the variation was from 0.85 at the hub to 0.60 at the tip. The performance of these high-camber and low-camber rotors was investigated to determine the angle-of-attack range as affected by a reduction in camber.

A velocity-diagram analysis indicated that the guide-vane turning has a significant effect on the rate of change of angle of attack with weight flow. These effects were checked experimentally by a comparison of the performance of the high-camber rotor with the original guide vanes, with guide vanes modified for reduced turning, and without guide vanes.

SYMBOLS

The following symbols are used in this report:

C_{L_O}	camber (lift coefficient of isolated airfoil)
M	Mach number
P	absolute total pressure, lb/sq ft
p	static pressure, lb/sq ft
r	radius, ft
U	rotor speed, ft/sec
V	absolute air velocity, ft/sec
W	weight flow, lb/sec
$W\frac{\sqrt{\theta}}{\delta}$	weight flow corrected to NACA standard sea-level pressure and temperature, lb/sec
z	axial distance
α	angle of attack, deg

[redacted]

β absolute inlet-air angle, angle between compressor axis and absolute air velocity, deg (for an inlet stage β equals guide-vane turning angle)

γ ratio of specific heats

δ ratio of inlet total pressure to NACA standard sea-level pressure

η average adiabatic temperature-rise efficiency

θ ratio of inlet total temperature to NACA standard sea-level temperature

ρ mass density, slugs/cu ft

σ solidity, ratio of chord length to distance between adjacent blades

φ blade-angle setting, angle between compressor axis and blade chord, deg

Subscripts:

0 depression tank

1 upstream of rotor

2 downstream of rotor

av average

e element

h hub

max maximum

t tip

z axial direction

θ tangential direction

Superscript:

' relative to rotor blade row

[redacted]

APPARATUS AND PROCEDURE

Compressor configurations. - The two rotor designs investigated were based on the same inlet-velocity distributions; therefore, the guide-vane assemblies used with both rotors in their original-stage configurations were identical in design. A measured guide-vane turning-angle distribution for the original guide vanes is shown in figure 1(a) as a function of radius ratio. Also plotted is a turning-angle distribution for the modified guide vanes. (The circular-arc sheet-metal guide vanes were modified for reduced turning angle by trimming the trailing edges.) On figure 1(b) are shown the details of the rotor-blade configurations: camber C_{l_0}, blade-angle setting φ, and solidity σ against radius ratio r/r_t. NACA 65-series compressor blade sections with 10 percent thickness and a chord of 1.31 inches were used. A stage, consisting of 19 rotor blades and 40 inlet guide vanes, had a hub-tip radius ratio at the rotor inlet of 0.50 and a rotor-tip diameter of 14 inches. Stator blades were not used because they were not considered necessary for this investigation and because additional sets would have been required for the investigations with modified guide vanes and without guide vanes.

Experimental setup. - The experimental equipment was similar to that described in reference 3. The compressor was driven by a 1500-horsepower dynamometer. Room air was drawn through a flat-plate orifice into a large depression tank. From the depression tank the air passed through a bellmouth inlet into the compressor, then through a large collector to an evacuated exhaust system. The desired inlet pressure and weight flow were set by means of valves located between the orifice tank and the depression tank, and between the collector and the exhaust system. A schematic diagram of the experimental setup is shown in figure 2.

Instrumentation. - Flow measurements were taken approximately 0.2-chord length upstream of the rotor blades and 0.6-chord length downstream of the rotor blades. Data were taken from tip to hub at five radial stations, a, b, c, d, and e, which were located at the centers of five equal radial increments across the passage upstream and downstream of the rotor blades. The location of these measuring stations is indicated in figure 3. Circumferential traverses of flow angle were made downstream of the guide vanes in order to locate the positions of the wakes at each of the radial measuring stations with the flow measurements then taken between the wakes.

The total-pressure losses across the guide vanes were obtained at each radial measuring station for several weight flows by means of circumferential wake surveys of total pressure. A guide-vane-loss calibration curve was prepared by plotting the total-pressure loss against corrected weight flow. The total pressure downstream of the guide vanes, then, equals the depression-tank total pressure P_0 minus the guide-vane loss.

The guide-vane wakes were found to pass through the rotor and to affect the measured flow angles downstream of the rotor; therefore, for each data point, the combination total-pressure and angle-measuring probe was traversed circumferentially until the total pressures indicated that the probe was in a flow region free of guide-vane wakes.

A summary of the number of probes and type of the instrumentation used is presented in the following table. It should be noted that, because of the negligible velocities in the depression tank, it was assumed that the depression tank static pressure p_0 is equal to P_0.

Station	Temperature	Total pressure	Static pressure	Angle
Inlet orifice	[a]4	Barometer reading	[b]2	--
Depression tank, 0	[a]4	[c]2	[c]2	--
Upstream of rotor, 1	--	--	[d]1	[e]1
Downstream of rotor, 2	[f]4	[g]1	[d]1	[g]1

[a]Iron-constantan thermocouple.
[b]Orifice static-pressure tap.
[c]Depression-tank static-pressure tap.
[d]Wedge-type static-pressure probe (fig. 4(a)).
[e]Claw total-head type yaw-measuring probe (fig. 4(b)).
[f]Five-tip double-stagnation type total-temperature rake (fig. 4(c)).
[g]Combination four-tube total-pressure rake and claw-type yaw-measuring probe (fig. 4(d)).

Radial surveys were made with probes shown in figures 4(a), 4(b), and 4(d).

Calculations

The average total-pressure ratio was based on a mass-flow-weighted average of the isentropic power input integrated across the flow passage (reference 4), that is

$$\left(\frac{P_2}{P_0}\right)_{av} = \left\{ \frac{\int_{r_{h,2}}^{r_t} \left[\left(\frac{P_2}{P_0}\right)^{\frac{\gamma-1}{\gamma}} - 1 \right] \rho_2 V_{z,2} r_2 \, dr}{\int_{r_{h,2}}^{r_t} \rho_2 V_{z,2} r_2 \, dr} + 1 \right\}^{\frac{\gamma}{\gamma-1}}$$

[redacted]

The average adiabatic temperature-rise efficiency was calculated from a mass-flow-weighted average of the total-temperature rise across the rotor and a mass-flow-weighted average of the isentropic power input (reference 4) as follows:

$$\eta = \frac{\int_{r_{h,2}}^{r_t} T_0 \left[\left(\frac{P_2}{P_0} \right)^{\frac{\gamma-1}{\gamma}} - 1 \right] \rho_2 V_{z,2} r_2 \, dr}{\int_{r_{h,2}}^{r_t} (T_2 - T_0) \, \rho_2 V_{z,2} r_2 \, dr}$$

Experimental procedure. - In general, a range of air flow was investigated at each speed from either the highest flow possible or that flow at which there was no pressure rise over the tip of the blade to a low flow at which the blades stalled near the tip; however, for the investigations with modified guide vanes at a speed of 552 feet per second and those without guide vanes, the air flows were further decreased to a point where very low over-all efficiency was indicated.

The performance of both rotors with the original guide vanes was investigated at corrected tip speeds of 552, 828, 1104, and 1214 feet per second corresponding to 50, 75, 100, and 110 percent of design speed. The investigations of the high-camber rotor with modified guide vanes were made at tip speeds of 552, 828, and 1104 feet per second; those without guide vanes were made at tip speeds of 546 feet per second. A rotor-blade failure terminated the tests without guide vanes before additional speeds could be investigated.

RESULTS AND DISCUSSION

Effects of Reduction in Camber

Over-all performance. - The over-all performance of each rotor with the original guide vanes, in terms of average pressure ratio and adiabatic temperature-rise efficiency plotted against corrected weight flow, is presented in figure 5 for the range of speeds investigated. For the design tip speed of 1104 feet per second, the following table summarizes the over-all performance of the high- and low-camber rotors:

	High-camber rotor			Low-camber rotor		
	P_2/P_0	η	$W\sqrt{\theta}/\delta$	P_2/P_0	η	$W\sqrt{\theta}/\delta$
Peak pressure ratio point	1.27	0.88	22.3	1.22	0.86	21.0
Peak efficiency point	1.265	.89	23.0	1.21	.90	22.4

[redacted]

The most apparent effect of the reduction in camber on the design-speed performance is the reduction in peak pressure ratio from 1.27 to 1.22.

The efficiency characteristics for a tip speed of 828 feet per second indicate that at this tip speed a slight extension of the weight-flow range accompanied the reduction in camber. For example, at a tip speed of 828 feet per second, the high-camber rotor has an efficiency of 0.85 or more for a range of 3.3 pounds per second of weight flow, while for the low-camber rotor, the corresponding range is 4.2 pounds per second. However, for a tip speed of 552 feet per second, no significant difference in weight-flow range is apparent.

Blade-element efficiency. - The blade-element efficiency characteristics of the high- and low-camber rotors are shown in figure 6 for tip speeds of 552 and 828 feet per second. A comparison of these efficiency characteristics indicates that for each of the rotors the over-all weight-flow range at an acceptable efficiency is limited by the performance of the tip region (measuring stations a and b) of the blades. At the low and high flows, the efficiencies measured at stations a and b (fig. 3) are much lower than for the rest of the blades. Also, the peak efficiencies measured at station a (0.77 to 0.81) are lower than at any other section.

These low peak efficiencies measured at the tip region show that at all flows investigated large losses occurred at this tip region. Several factors probably contribute to these losses, including tip clearance effects and casing boundary-layer losses. Also, the radial pressure gradient established by the rotating flow imposes a larger static-pressure rise at the tip region than at the other sections. It is possible, therefore, that local values of the blade-surface static-pressure gradient dp/dz would become excessive and lead to flow separation with consequent high losses.

Although data are not available for the evaluation of the local blade-surface pressure gradient, a high value of over-all static-pressure rise across the rotor probably corresponds to a high surface-pressure gradient. The pressure rise that can be tolerated across a blade row is related in part to the inlet relative velocity. The ratio of the pressure rise across the rotor to the pressure equivalent of the inlet relative velocity $(p_2-p_1)/(P_1'-p_1)$ may then constitute a parameter that will help correlate the tip-efficiency characteristics with those of the other blade sections. The limiting value of the pressure-rise parameter is probably smaller at the tip than at the other blade sections because of tip clearance and boundary-layer effects. Values of this parameter are plotted against corrected weight flow for the high- and low-camber rotors in figure 7 for a tip speed of 828 feet per second.

The curves indicate that the static-pressure-rise characteristics are very similar for both rotors. In both cases, the pressure-rise parameter is highest at the tip measuring station. Corresponding peak values of efficiency and pressure-rise parameter are tabulated as follows for measuring stations a and b.

Measuring station	High-camber rotor		Low-camber rotor	
	η_e	$\frac{p_2-p_1}{p_1'-p_1}$	η_e	$\frac{p_2-p_1}{p_1'-p_1}$
a	0.765	0.43	0.805	0.39
b	.895	.40	.955	.365

The difference in peak values of the pressure-rise parameter is small compared with the large difference in peak efficiency. Probably the limiting value of the parameter for the tip region (which would be smaller than for the other blade sections because of tip clearance and boundary-layer effects) has been exceeded.

A possible additional explanation for this trend would be that, in the case of the tip measuring station, the peak value of the local pressure gradient dp/dz is appreciably higher than that at station b, even though the over-all pressure-rise coefficients differ only slightly.

As the flow passes between the blades, the pressure of an incremental mass of gas rises in accord with the increase in local flow area. In the case of a two-dimensional cascade of blades, the factors of blade shape, blade stagger angle, solidity, and turning angle determine the over-all dimensionless pressure-rise parameter. But in the case of a rotating blade row, the pressure must also balance the centrifugal force of the rotating mass of gas as well as the radial accelerations that are present. For no radial flow, the radial pressure gradient is given by the simplified radial-equilibrium equation $\frac{1}{\rho}\frac{dp}{dr} = \frac{V_\theta^2}{r}$. At the tip region of a rotor where the centrifugal force of the rotating flow is high because of high values of tangential velocity, the required pressure downstream of the blade row can be obtained only by an enlargement of the flow area in the radial direction. The ratios of downstream-to-upstream axial velocity for the high-camber and low-camber rotors are shown in figure 8 for a tip speed of 828 feet per second. The general decrease in axial velocity at the tip and increase at the hub indicate that, at all flows investigated, the flow shifted radially towards the hub. Data are not available for the evaluation directly of the rate of increase of flow area or the pressure gradient dp/dz as functions of axial distance. However, local values of the pressure gradient probably could be appreciably different from the average values indicated by the over-all pressure-rise coefficient. Thus, the enlargement of the local flow area at the tip region may contribute to a premature flow separation from the blades with consequent high tip losses.

[redacted]

Effect of camber on range. - The blade-element efficiency, pressure-rise, and radial-flow characteristics have indicated that the change in blade camber (of values of C_{L_0} from 0.87 to 0.60 at the tip and from 1.69 to 0.85 at the hub) has slight effect on range. In terms of the pressure parameter $(p_2-p_1)/P_1'-p_1)$, the reduction in camber represents an attempt to relieve the diffusion by reducing the value of the numerator, the static-pressure rise. However, apparently little improvement can be realized by this procedure without a large sacrifice in total-pressure ratio. The maximum local values of pressure gradient dp/dz may be only slightly affected because the axial-velocity characteristics (fig. 8) indicate that similar radial-flow characteristics were encountered with both rotors.

Effects of Reduction in Guide-Vane Turning

Velocity-diagram analysis. - A typical rotor velocity diagram is shown in figure 9. A study of this velocity diagram yields an expression for the rate of change of angle of attack with respect to axial velocity as a function of wheel speed, relative inlet angle, and absolute inlet angle. From the diagram

$$\tan \beta' = \tan (\varphi + \alpha) = \frac{U - V_z \tan \beta}{V_z} = \frac{U}{V_z} - \tan \beta$$

The derivative with respect to V_z yields

$$\sec^2 \beta' \frac{d\alpha}{dV_z} = - \frac{U}{V_z{}^2}$$

(because β and φ are constant at a given radius neglecting Mach number effects on β).

V_z can be eliminated by appropriate substitutions determined from the vector diagram to yield

$$\frac{d\alpha}{dV_z} = - \frac{1}{U} (\sin \beta' + \cos \beta' \tan \beta)^2$$

The expression shows that, at a given radius and a fixed relative inlet-air angle, a decreased guide-vane turning β should cause a decrease in the absolute magnitude of the rate of change of angle of attack with respect to axial velocity (hence with weight flow) and extend the weight-flow range at good efficiency.

Modified guide vanes. - The guide vanes were modified for reduced turning (by trimming the trailing edges); typical measured turning angles for the original and modified guide vanes are shown in figure 1(a). The guide-vane turning was reduced more near the hub than near the tip because it was desired to increase the hub angles of attack for a given angle of attack at the tip in order to better match all blade elements. The blade-element-efficiency characteristics of the high-camber rotor (fig. 6) show that even at the lowest flow investigated the peak efficiency was not reached at the hub region. It was desired to check the effects on range of decreased guide-vane turning and to improve the radial-blade-element matching so that the peak efficiencies at all the measuring stations would occur at approximately the same weight flow.

Over-all performance. - The over-all performance of the high-camber rotor with the modified guide vanes is shown in figure 10 as plots of average total-pressure ratio and adiabatic temperature-rise efficiency against corrected weight flow for tip speeds of 552, 828, and 1104 feet per second. In the following discussion the term "original stage" refers to the high-camber rotor with original guide vanes; the term "modified" stage" refers to the high-camber rotor with modified guide vanes.

The peak efficiencies at tip speeds of 552 and 828 feet per second are slightly higher for operation with the modified guide vanes than with the original guide vanes (fig. 5) but, at a tip speed of 1104 feet per second, a marked drop in efficiency is noted. The peak pressure ratios are higher for the modified stage than for the original stage. Comparative performance data are tabulated as follows:

	Original guide vanes			Modified guide vanes		
U_t	552	828	1104	552	828	1104
η_{max}	0.88	0.89	0.89	0.90	0.915	0.80
$(P_2/P_0)_{max}$	1.055	1.145	1.27	1.07	1.17	1.31

At a tip speed of 828 feet per second, the weight-flow range was increased from 3.3 pounds per second at an efficiency of 0.85 for the original stage to 6.2 pounds per second for the modified stage. The corresponding weight-flow ranges at a tip speed of 552 feet per second were 2.5 and 4.05 pounds per second for the original stage and the modified stage, respectively. Part of this increase in range (where range is defined at some specified value of efficiency, in this case 0.85) is the result of the increase in peak efficiency at the low speeds. The

weight-flow range can also be compared for a given percentage reduction from the peak efficiency. On this basis, the weight-flow range for an efficiency 0.04 less than the peak efficiency was increased, at a tip speed of 828 feet per second, from 3.3 pounds per second for the original stage to 4.3 pounds per second for the modified stage. The corresponding ranges at a tip speed of 552 feet per second were 2.9 and 4.0 pounds per second, respectively. (Determination of the range of the original stage at 552 ft/sec at an efficiency of 0.84 required a slight extrapolation of the efficiency curve.)

Blade-element efficiency. - The blade-element-efficiency characteristics of the high-camber rotor with modified guide vanes are plotted in figure 11 for the tip speeds investigated. Also plotted are the relative inlet Mach numbers as a function of corrected weight flow for a tip speed of 1104 feet per second.

For a tip speed of 1104 feet per second, the curves indicate low efficiencies, especially for station d. The Mach number characteristics show that for all flows investigated relative inlet Mach numbers were over 0.77 for the portion of the blade from the mean radius to the hub and the highest Mach numbers were measured at station d. Cascade investigations of the NACA 65(12)-10 blade section have shown that total-pressure losses increase rapidly as the inlet relative Mach number exceeds a value of about 0.75 (fig. 10 of reference 6). A similar behavior might be expected of NACA 65-series blades using values of camber slightly higher or lower than that used for the investigation of reference 6. The range of cambers used in the high-camber rotor ($0.87 < C_{L_0} < 1.69$) includes the value ($C_{L_0} = 1.2$) used for the cascade investigations; thus, the low value of peak over-all efficiency noted in figure 10 for a tip speed of 1104 feet per second is probably a Mach number effect resulting in high losses in the hub region of the rotor blades.

The blade-element-efficiency characteristics for tip speeds of 552 and 828 feet per second indicate improved blade-element matching because the peak efficiencies for all the blade elements occur at approximately the same weight flow. This improved blade-element matching accounts for the slight increase in peak over-all efficiency that was noted for the modified stage as compared with the original stage and accounts for part of the extension of weight-flow range that accompanied the operation with modified guide vanes.

Static-pressure-rise characteristics. - The efficiency characteristics for the original and modified stages are similar in that the tip-region performance limits the range at reduced speeds in both cases; also, the peak efficiencies are low at the tip. The static-pressure-rise characteristics for the original and modified stages are shown in

figure 12, where the pressure coefficient is plotted against angle of attack for a tip speed of 828 feet per second. At a given angle of attack, approximately the same pressure coefficient is indicated for both stages at measuring station a. This is to be expected because the tip-inlet conditions were practically the same for the original and modified stages.

The axial-velocity ratios for the modified guide vanes (fig. 13) indicate a trend similar to that noted for operation with the original guide vanes (fig. 8). The axial velocity decreases at the tip and increases at the hub, a fact that indicates a radial shift in flow towards the hub. The tip-region conditions of radial shift in flow and large static-pressure rise have not been improved, and the high tip losses characteristic of the original stage are also encountered with the modified stage.

Rate of change of angle of attack with weight flow. - The principal effect that was expected, on the basis of the velocity-diagram analysis, from the decreased guide-vane turning was a general reduction in the magnitude of the rate of change of angle of attack with respect to weight flow for each of the blade elements except at the extreme tip. Figure 14 shows angles of attack against corrected weight flow for the original and modified stages at a tip speed of 828 feet per second. The curves indicate that the expected effect on the rate of change of angle of attack with weight flow was actually obtained. Measured values of the slopes of these curves $\frac{d\alpha}{dw\frac{\sqrt{\theta}}{\delta}}$ are tabulated as follows for the peak efficiency point:

Radial position	Original guide vanes (deg/(lb)(sec))	Modified guide vanes (deg/(lb)(sec))
a	-2.49	-2.45
c	-2.02	-1.30
e	-1.52	-1.00

This general reduction in the rate of change of angle of attack with weight flow was one of the reasons that an appreciable extension of the weight-flow range was realized for the modified stage even though no improvement was noted in the static-pressure rise at the tip region.

Discussion of tip-stall problem. - High guide-vane turnings have been used for inlet stages in order to combine a high tip speed with a subsonic Mach number limit. The result is that the values of tangential

velocity downstream of the rotor are high. The simplified radial-equilibrium equation $\frac{1}{\rho}\frac{dp}{dr} = \frac{V_\theta^2}{r}$ indicates that a large static-pressure gradient must exist to balance the centrifugal force of a flow with a large tangential component of velocity. The resulting high static pressure at the tip requires that the flow shifts radially towards the hub as it passes through the rotor with the possible separation difficulties discussed in the section Effects of Reduction in Camber. Very low guide-vane turning will reduce the whirl velocity downstream of the rotor for a fixed turning angle and should tend to reduce the static pressure at the tip and thereby relieve the radial shift in flow.

Rotor operation without guide vanes. - As a check on the foregoing ideas, the high-camber rotor was operated with the guide vanes removed. Only a speed of 546 feet per second was investigated after which a rotor-blade failure terminated the tests.

Over-all performance without guide vanes. - The over-all performance of the rotor without guide vanes is presented in figure 15. The data indicate a high peak efficiency (0.94 at a weight flow of 18 lb/sec) and a peak pressure ratio of 1.10 at a weight flow of 14.25 pounds per second. The peak pressure ratio of 1.10 is much higher than that measured with the original guide vanes (1.055 at a tip speed of 552 ft/sec). This represents an increase of 78 percent in the isentropic power input and is the result of operation with increased relative stagnation conditions.

The weight-flow range (10.5 lb/sec at an efficiency of 0.85) is much wider than that of the original stage; in fact, it extends over most of the weight flows investigated for the original stage at tip speeds of 552, 828, and 1104 feet per second. Part of this extension in range (as defined for a given minimum efficiency) is the result of increased peak efficiency, but it is the result mostly of the direct effect of the decreased absolute inlet-air angles on the rate of change of angle of attack with weight flow.

Values of actual angle of attack are plotted in figure 16 against corrected weight flow for the high-camber rotor with the original guide vanes at tip speed of 828 feet per second and without guide vanes at 546 feet per second. The tip speeds of 828 feet per second and 546 feet per second for the original stage and the case without guide vanes, respectively, represent operation in approximately the same relative Mach number range. Measured values of the slopes $\frac{d\alpha}{dw\,\frac{\sqrt{\theta}}{\delta}}$ are tabulated as follows for the peak efficiency points:

Radial position	Original guide vanes (deg/(lb)(sec))	Without guide vanes (deg/(lb)(sec))
a	-2.49	-1.48
c	-2.02	-1.62
e	-1.52	-1.70

The greatest decrease in the magnitude of rate of change of angle of attack with weight flow took place at the tip region. Because the tip-region performance limited the range for the original stage, this decrease in $\frac{d\alpha}{dw\frac{\sqrt{\theta}}{\delta}}$ greatly extended the over-all weight-flow range.

Blade-element efficiency without guide vanes. - The blade-element efficiency characteristics (fig. 17) reveal two interesting features: the tip-region maximum efficiency (0.91 at station a) is high, and its weight-flow range approaches that of the other blade elements.

The adiabatic temperature-rise efficiency whereby the stages are rated is computed from the total-pressure rise from the depression tank to the measuring station downstream of the rotor, as described in the section APPARATUS AND PROCEDURE. Guide-vane losses therefore detract from the original values of the efficiency. The question arises: Do guide-vane losses at the tip account for the low efficiency of the original stage? Calculations based on wake surveys downstream of the guide vanes indicate that the peak efficiency of 0.765 at station a for the original stage at a tip speed of 828 feet per second becomes 0.805 if based on the total-pressure rise from the station after the guide vanes to the station downstream of the rotor. Thus, the high tip efficiency for the investigations without guide vanes cannot be wholly accounted for by the absence of guide-vane losses.

Static-pressure-rise characteristics without guide vanes. - The more probable reason for the high tip efficiency is that a lower rate of diffusion of relative velocity was required across the rotor tip for the configuration without guide vanes than for the original stage. Values of the pressure parameter are plotted against angle of attack for the high-camber rotor with original guide vanes and without guide vanes in figure 18. The curves indicate that at any given angle of attack the pressure parameter is less at station a for the configuration without guide vanes than for the original stage until the stall point is reached where the curves peak. The axial-velocity ratios (fig. 19) indicate that the pressure rise across the rotor at the tip region was

obtained without the radial shift in flow that was noted for operation with guide vanes (figs. 8 and 13). At the peak-efficiency point ($w\sqrt{\theta}/\delta$ = 18 lb/sec), for example, all the values of $V_{z,2}/V_{z,1}$ lie between 1.05 and 1.07. Thus the flow is very nearly two dimensional and the local values of blade-surface-pressure gradient dp/dz are probably similar to those measured in two-dimensional-cascade investigations.

Angle-of-attack range without guide vanes. - Values of adiabatic temperature-rise efficiency are plotted against angle of attack at measuring station a in figure 20 for the three configurations of the high-camber rotor. A much wider range of angle of attack is indicated for the configuration without guide vanes than for the other configurations at any usable value of efficiency. The indication is that the more favorable rate of pressure rise permitted operation over an appreciable angle-of-attack range without excessive separation of the flow from the blade suction surface.

Mach number effect without guide vanes. - The use of high tip speeds, limited by turbine-stress considerations, in conjunction with low guide-vane turning will result in high absolute and relative Mach numbers. For relative Mach numbers over 0.75 to 0.80 a rapid increase in total-pressure losses is encountered with the NACA 65(12)-10 compressor blades (reference 5). A similar effect can be expected for NACA 65-series blades with other cambers. However, with the proper choice of blade shape, it has been shown experimentally that low hub-tip-ratio designs can be operated in the transonic Mach number range with good efficiency (reference 6). At present, information concerning the angle-of-attack range of these transonic airfoil sections when operated at low Mach numbers (low speeds) is not available.

SUMMARY OF RESULTS

The results of the investigation of the effects of camber and absolute flow angle on the range of a single-stage compressor can be summarized as follows:

1. The narrow usable weight-flow range exhibited by inlet-stage-compressor designs that feature high guide-vane turning in order to combine a subsonic Mach number limit with high tip speed was caused mainly by two factors: (a) high absolute inlet-air angles resulted in a large rate of change of angle of attack with axial velocity and (b) the comparatively low relative inlet velocities and the large static-pressure gradient downstream of the rotor resulted in an excessive pressure rise at the rotor-tip region and in a radial shift in flow towards the hub. The high pressure rise and radial shift in flow may cause an excessive local pressure gradient on the blade surface. Both effects are most

severe at the tip region where the additional effects of tip clearance and casing boundary layer might help to lead to a premature flow separation. Hence, the over-all range was limited by the three-dimensional stall characteristics of this portion of the blade.

2. Decreased blade camber had very little effect on weight-flow range because it affected the pressure-rise characteristics and radial shift in flow only slightly. A large reduction in camber, hence in total-pressure ratio, would be required in order to realize any appreciable reduction in the static-pressure rise where the inlet conditions are the result of high guide-vane turning.

3. Reduction in the magnitude of guide-vane turning and elimination of the guide vanes resulted in a large decrease in the rate of change of angle of attack with axial velocity. Furthermore, for the rotor configuration investigated, the zero guide-vane turning established a downstream static-pressure gradient that required a less severe rate of pressure rise at the rotor tip and the flow did not shift in a radial direction. The results of this low pressure coefficient at the tip and approximately two-dimensional flow were high peak blade-element efficiency (reflected in high over-all efficiency) and increased usable range of angle of attack.

Lewis Flight Propulsion Laboratory
National Advisory Committee for Aeronautics
Cleveland, Ohio

REFERENCES

1. Finger, H. B., and Dugan, James F., Jr.: Analysis of Stage Matching and Off-Design Performance in a Multistage Axial-Flow Compressor. NACA RM E52D07.

2. Herrig, L. Joseph, Emery, James C., and Erwin, John R.: Systematic Two-Dimensional Cascade Tests of NACA 65-Series Compressor Blades at Low Speeds. NACA RM L51G31, 1951.

3. Burtt, Jack R.: Investigation of Performance of Typical Inlet Stage of Multistage Axial-Flow Compressor. NACA RM E9E13, 1949.

4. Mankuta, Harry, and Guentert, Donald C.: Investigation of Performance of Single-Stage Axial-Flow Compressor Using NACA 5509-34 Blade Section. NACA RM E8F30, 1948.

5. Briggs, William B.: Effect of Mach Number on the Flow and Application of Compressibility Corrections in a Two-Dimensional Subsonic-Transonic Compressor Cascade Having Varied Porous-Wall Suction at the Blade Tips. NACA TN 2649, 1952.

6. Lieblein, Seymour, Lewis, George W., Jr., and Sandercock, Donald M.: Experimental Investigation of an Axial-Flow Compressor Inlet Stage Operating at Transonic Relative Inlet Mach Numbers. I - Over-All Performance of Stage with Transonic Rotor and Subsonic Stators up to Rotor Relative Mach Number of 1.1. NACA RM E52A24, 1952.

[redacted]

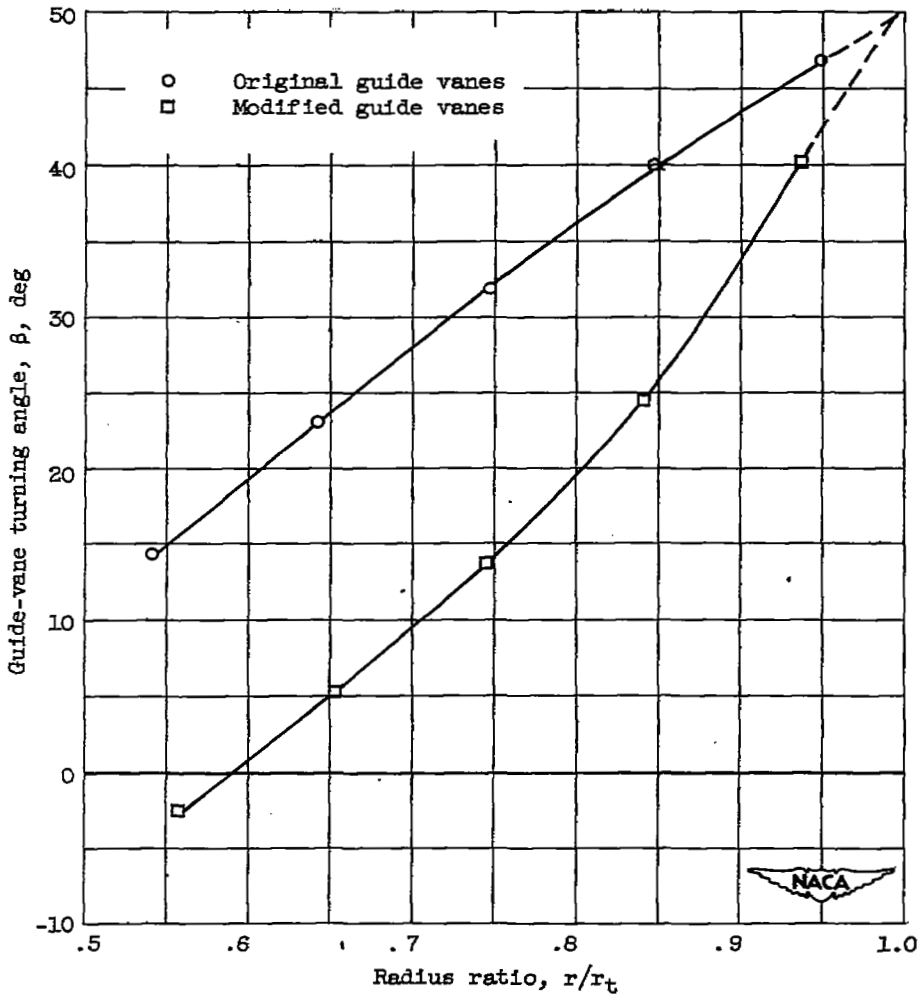

(a) Variation of guide-vane turning angle with radius ratio.

Figure 1. - Characteristics of rotor-blade configuration.

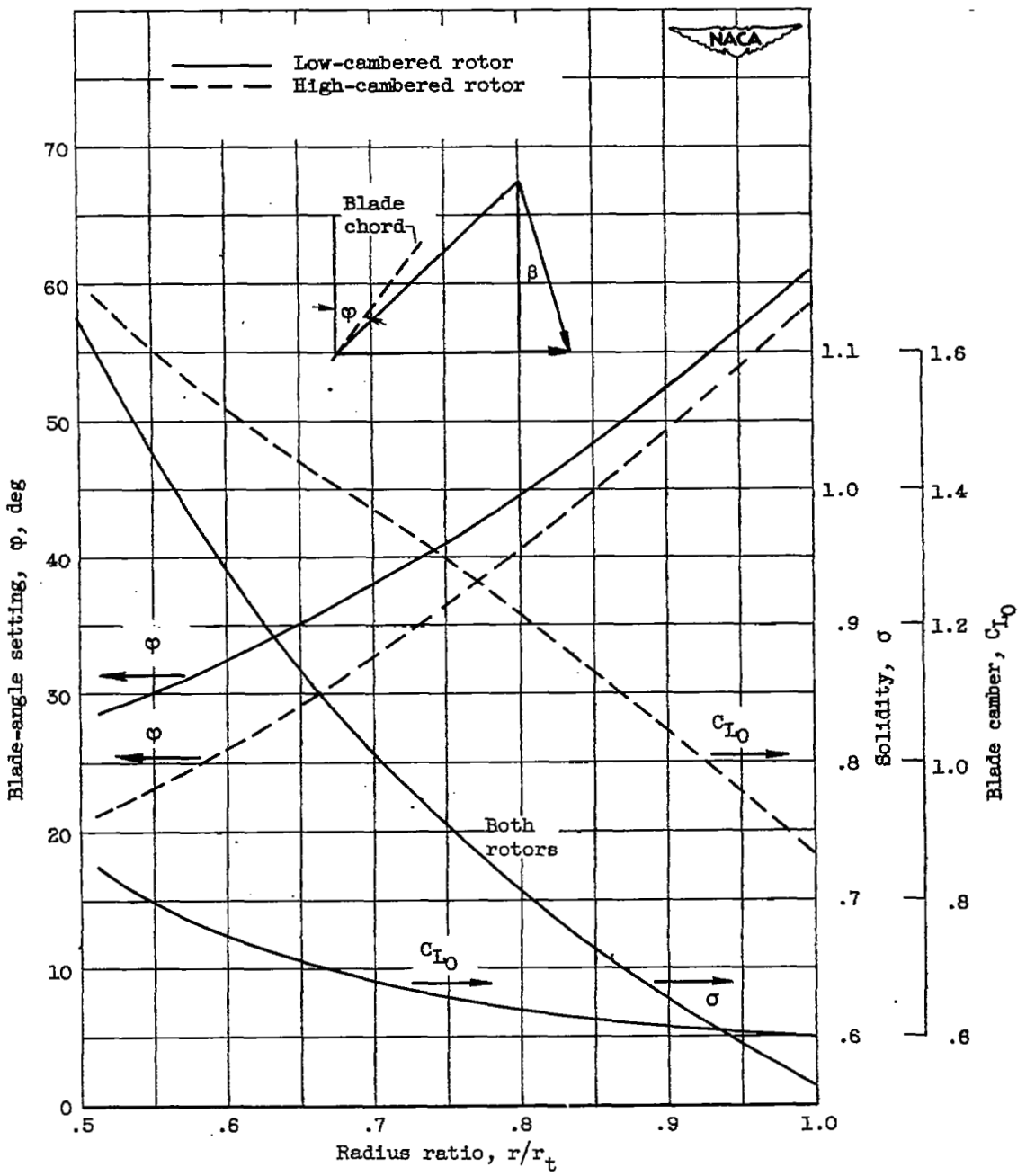

(b) Variation of blade-angle setting with radius ratio.

Figure 1. - Concluded. Characteristics of rotor-blade configuration.

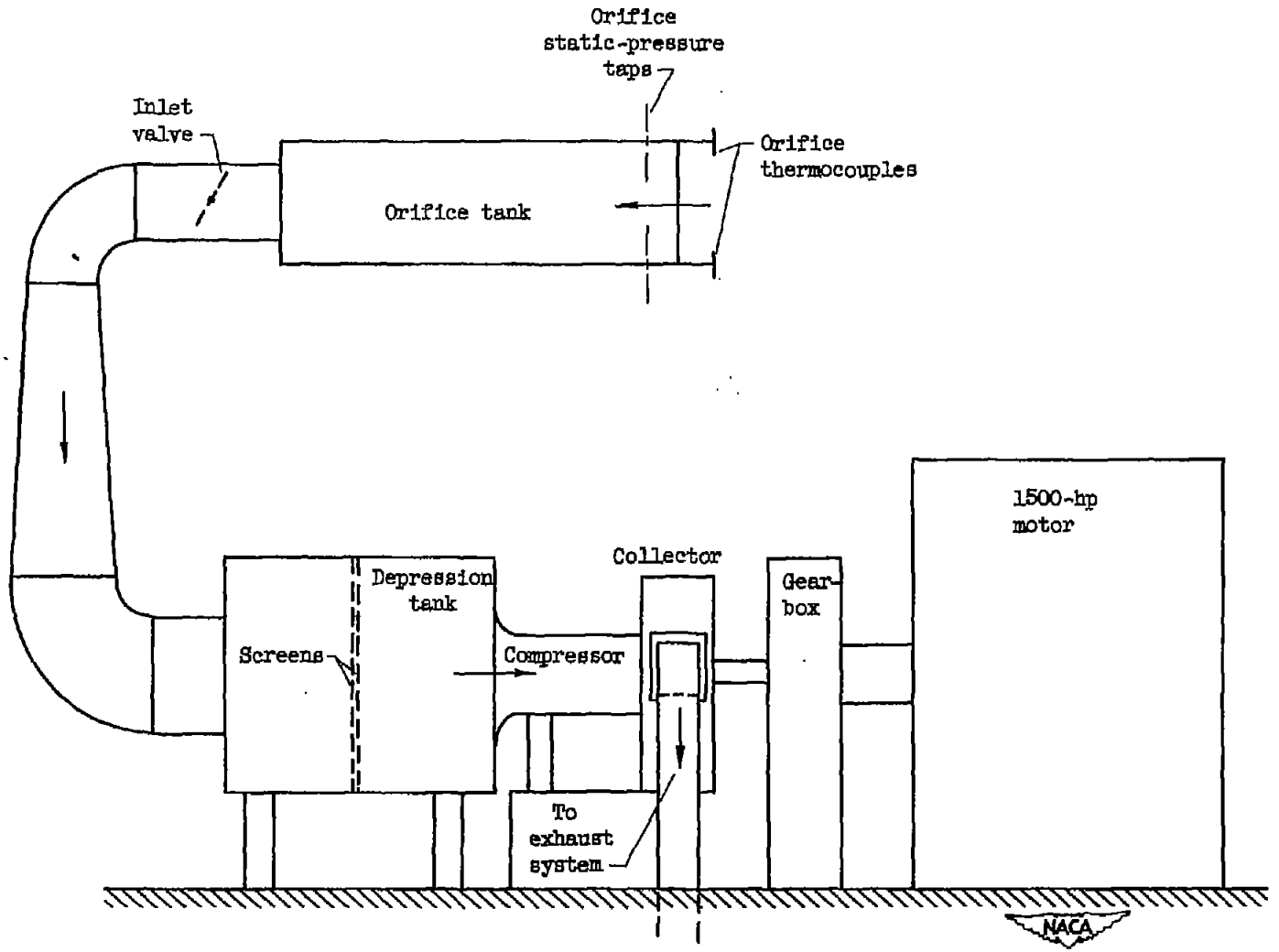

Figure 2. - Experimental setup.

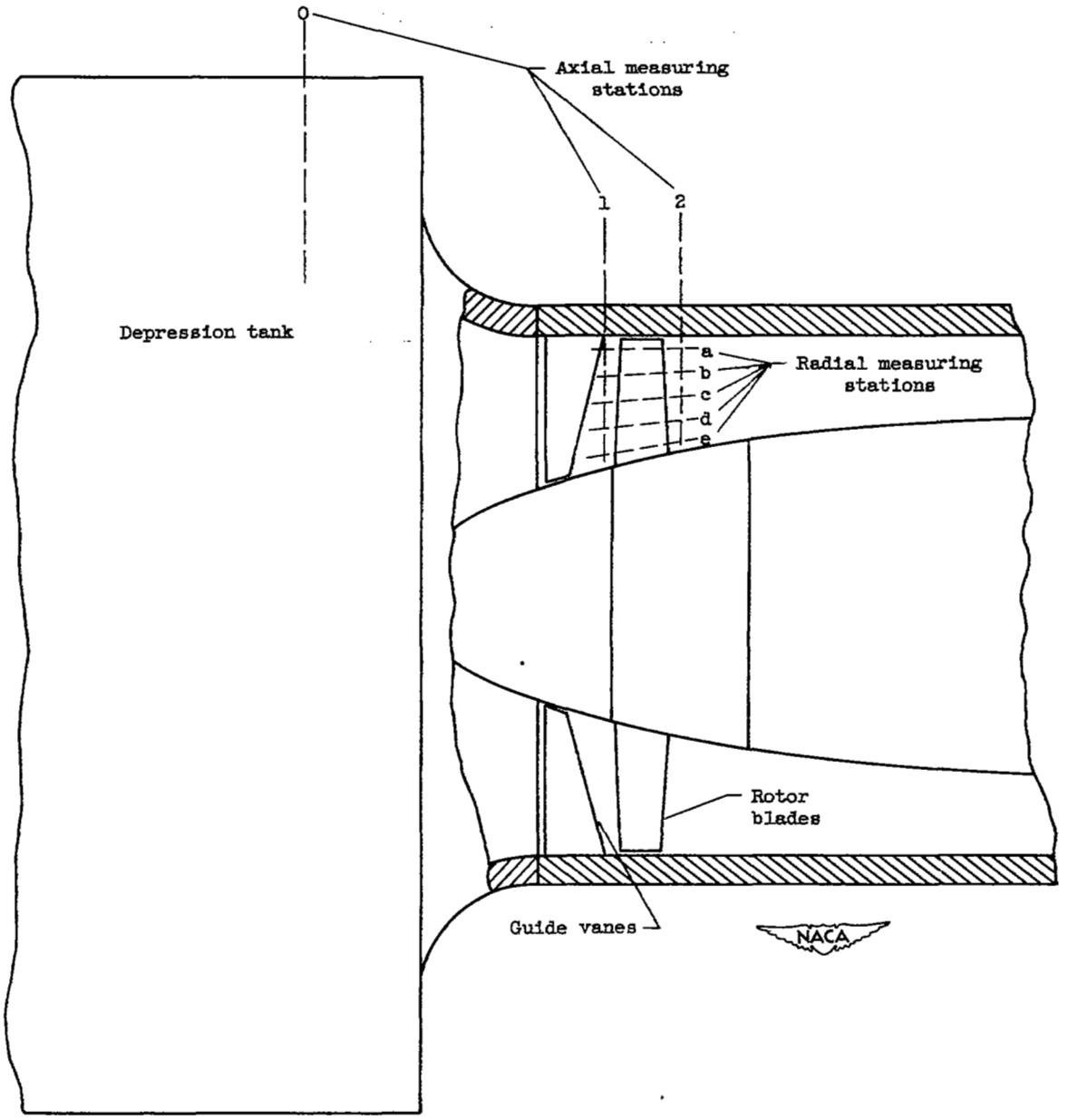

Figure 3. - Experimental compressor.

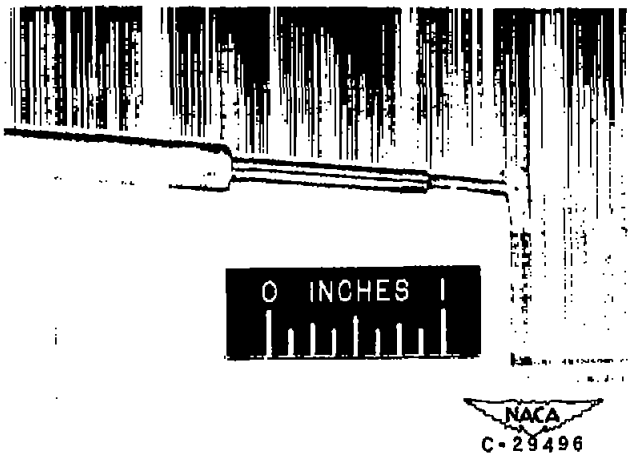

(a) Wedge-type static-pressure probe.

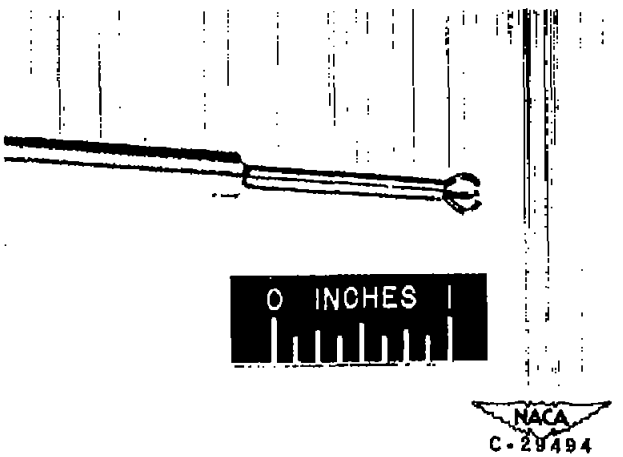

(b) Claw total-pressure type yaw-measuring probe.

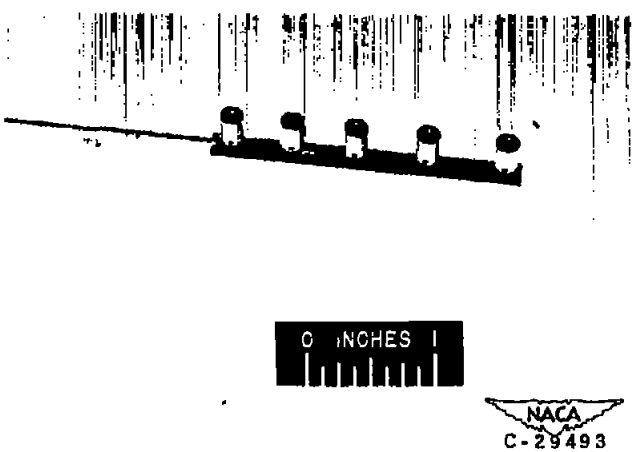

(c) Five-tip double-stagnation-type total-temperature rake.

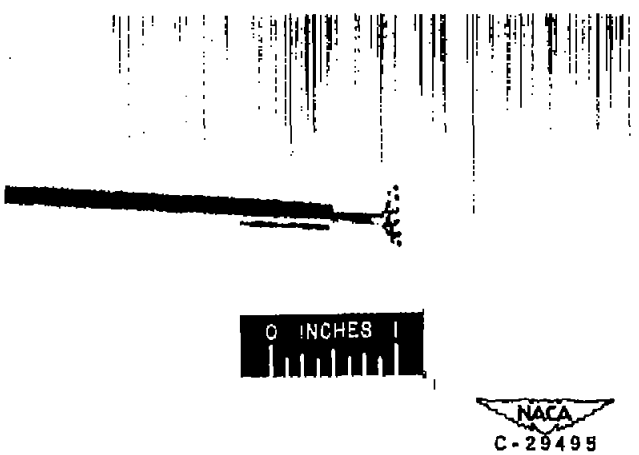

(d) Combination total-pressure yaw-measuring probe.

Figure 4. - Instrument probes.

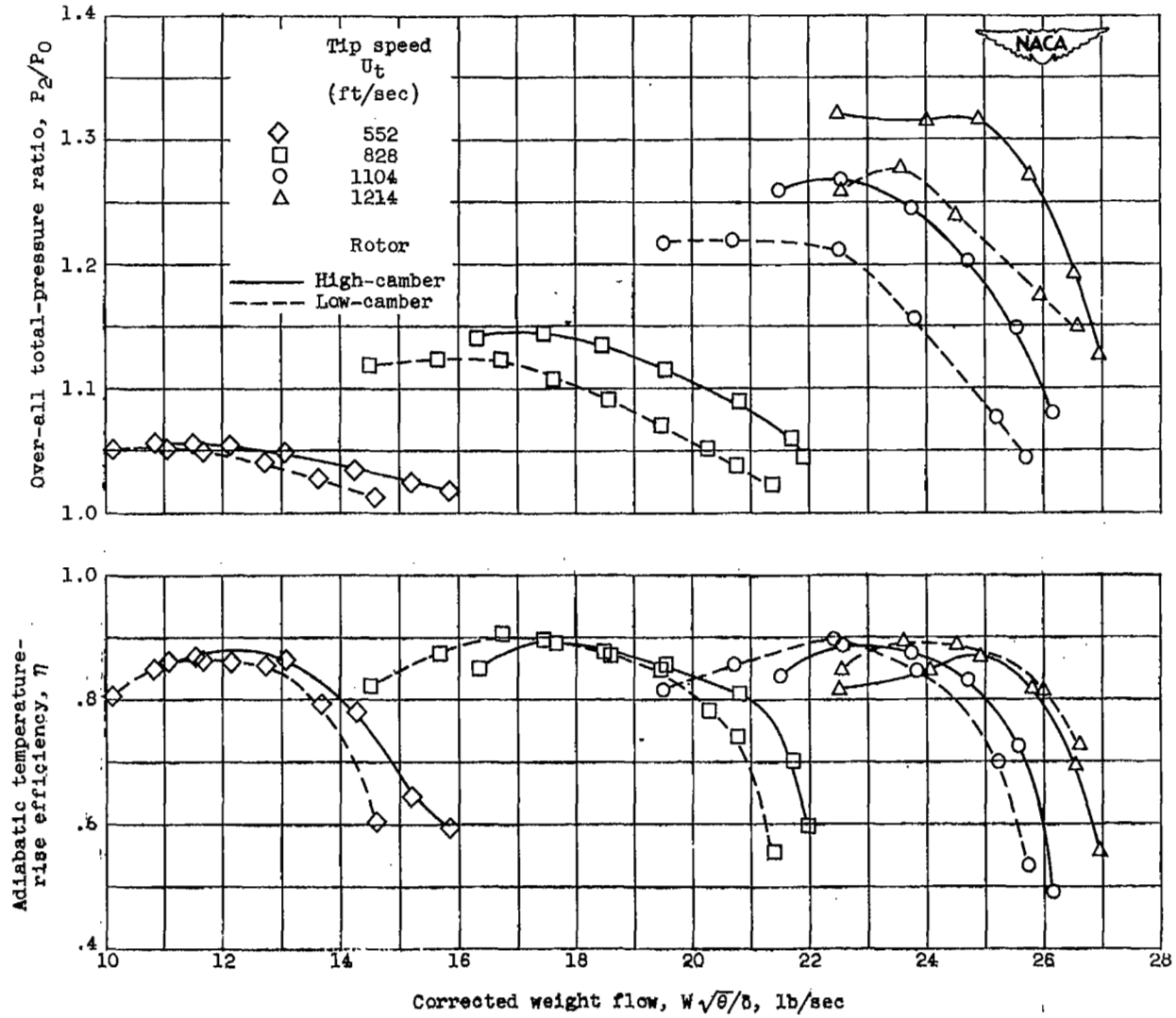

Figure 5. - Over-all performances of both rotors with original guide vanes.

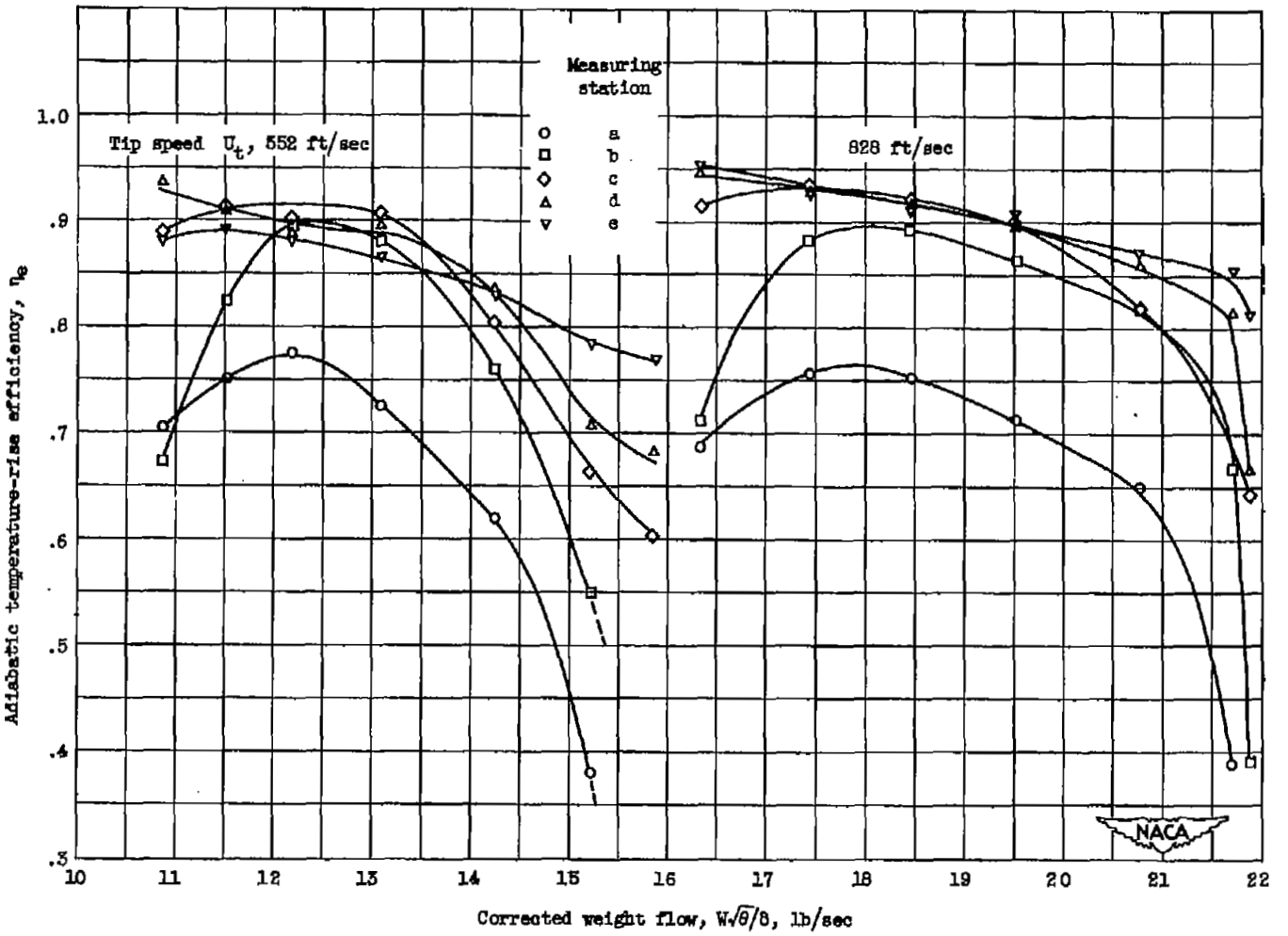

(a) High-camber rotor.

Figure 6. - Blade-element efficiency characteristics of both rotors with original guide vanes.

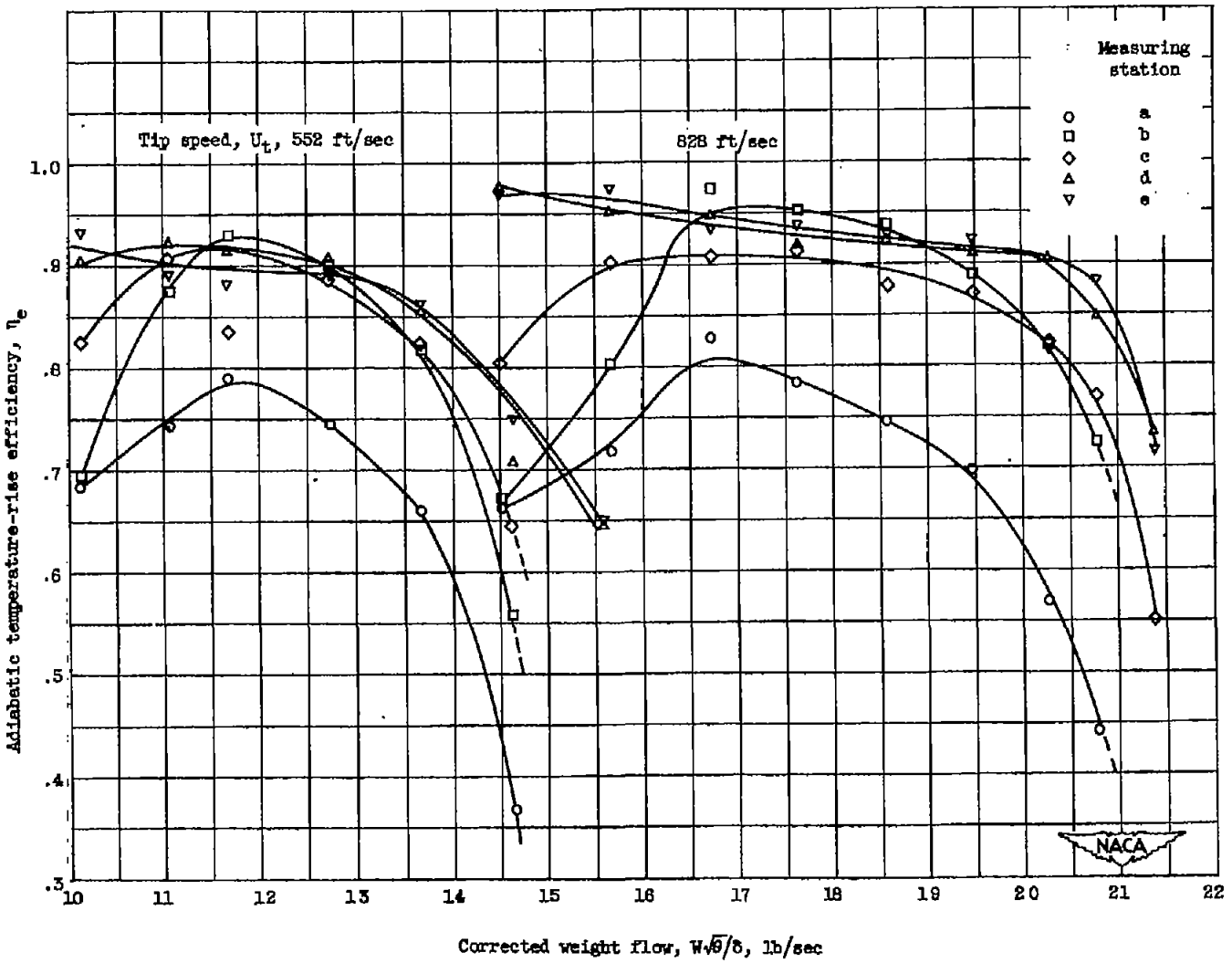

(b) Low-camber rotor.

Figure 6. - Concluded. Blade-element efficiency characteristics of both rotors with original guide vanes.

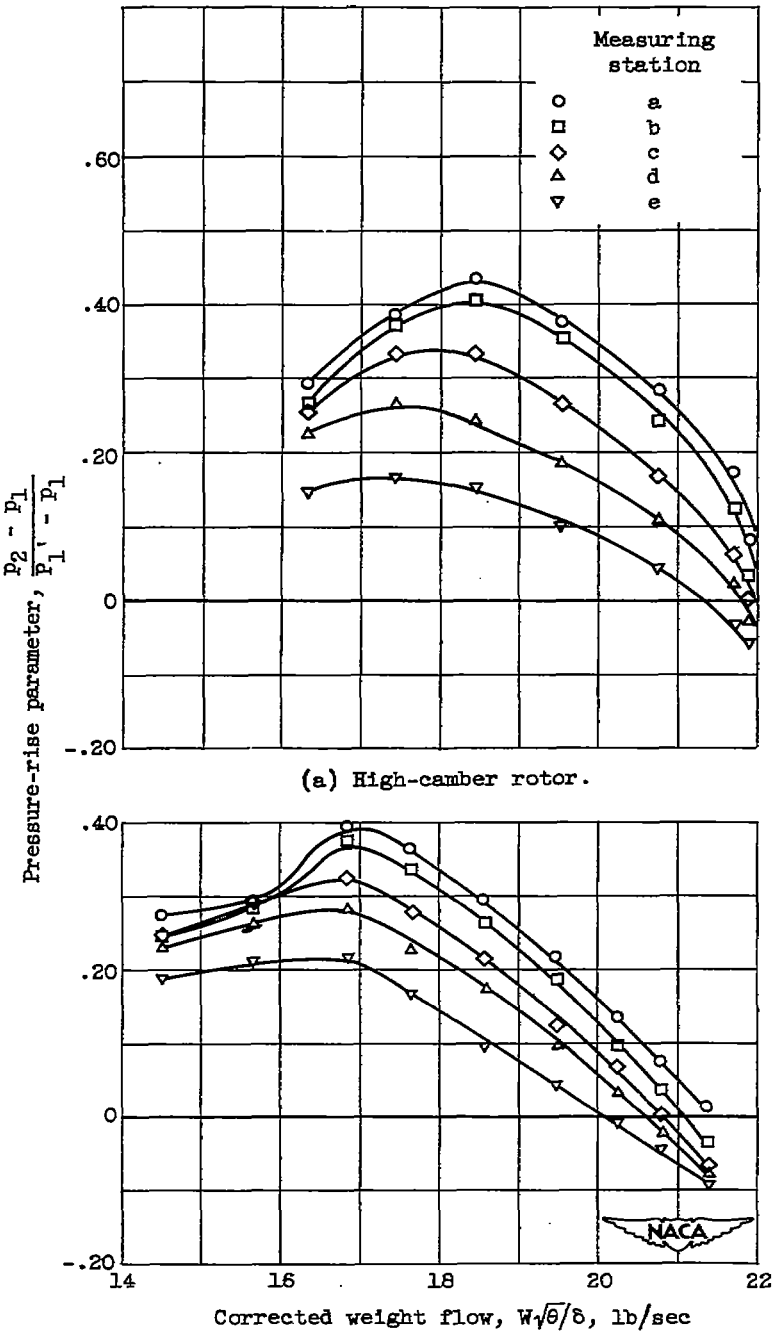

(a) High-camber rotor.

(b) Low-camber rotor.

Figure 7. - Variation of pressure-rise parameter with corrected weight flow of both rotors with original guide vanes. Tip speed U_t, 828 feet per second.

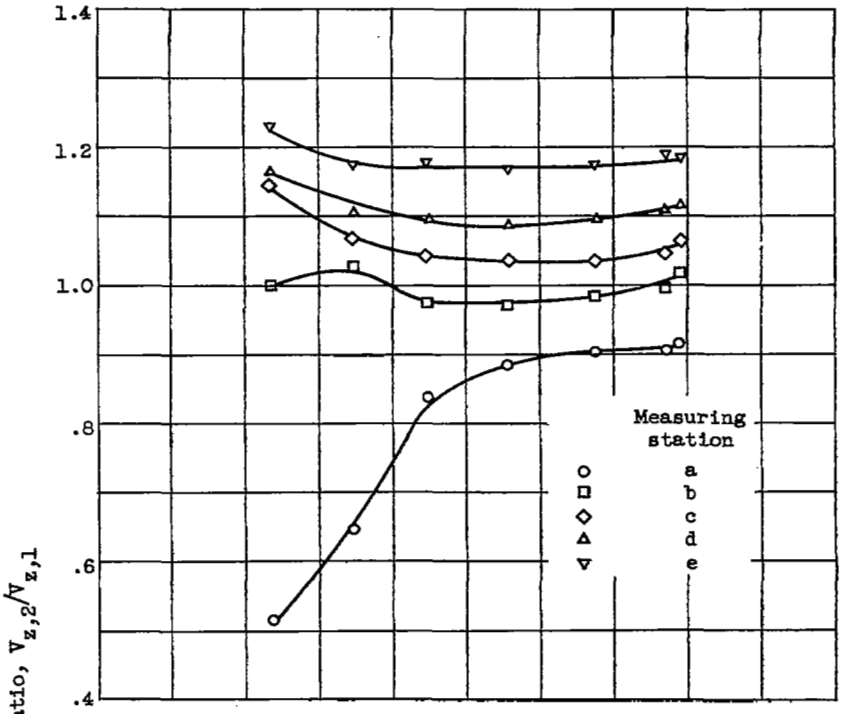

(a) High-camber rotor.

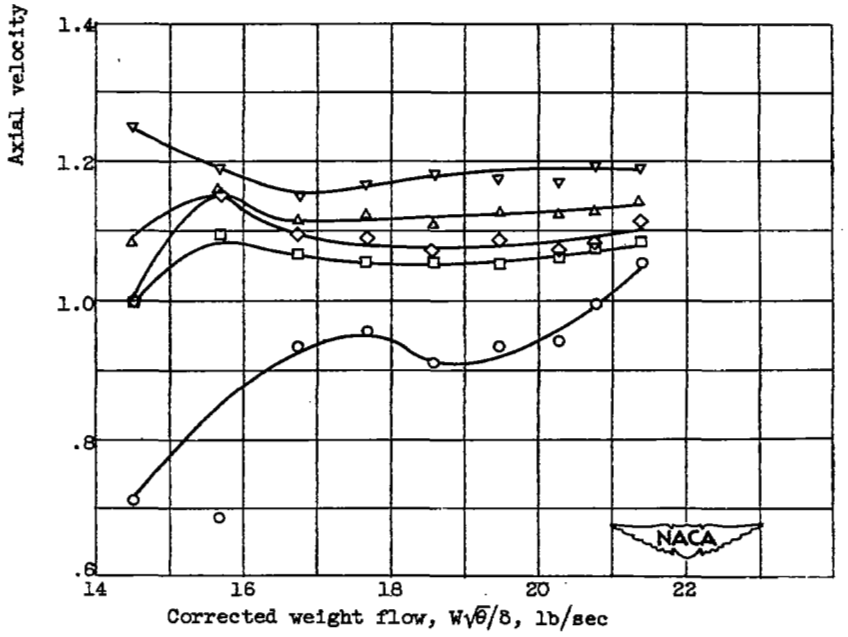

(b) Low-camber rotor.

Figure 8. - Variation of axial-velocity ratio with equivalent weight flow for both rotors. Tip speed U_t, 828 feet per second.

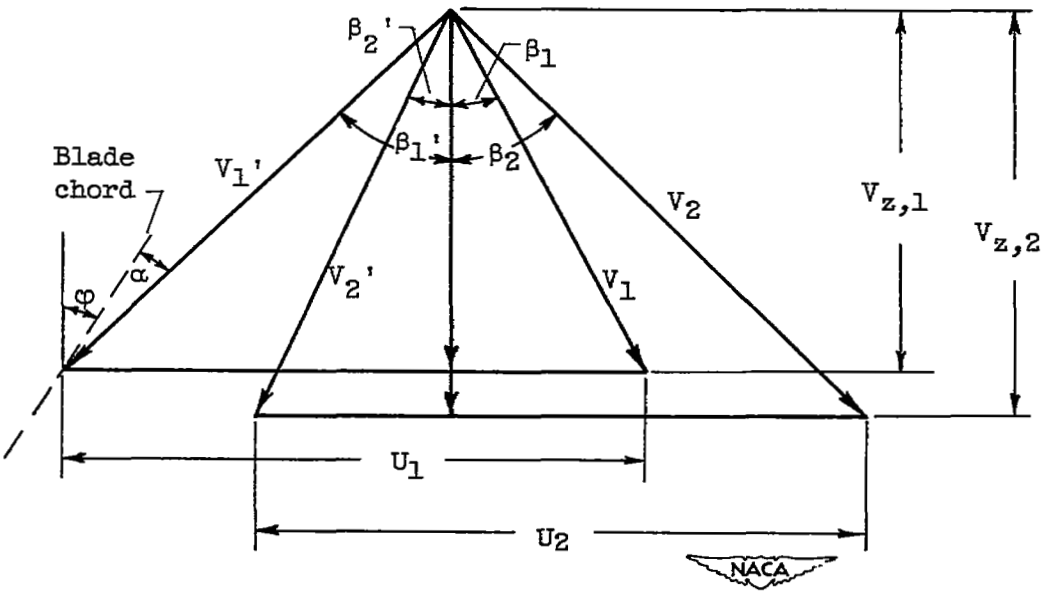

Figure 9. - Typical rotor velocity diagram.

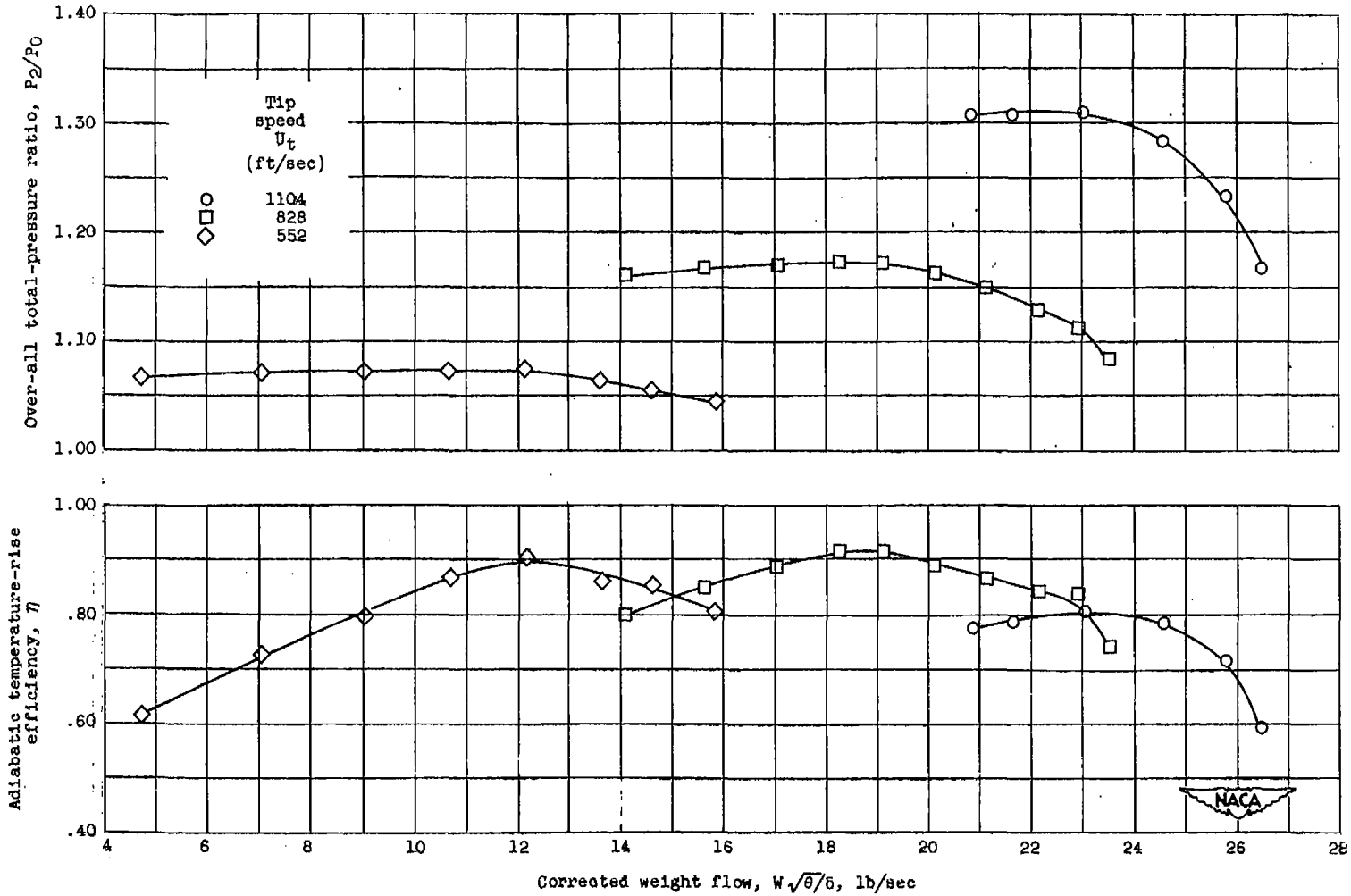

Figure 10. - Over-all performances of high-camber rotor with modified guide vanes.

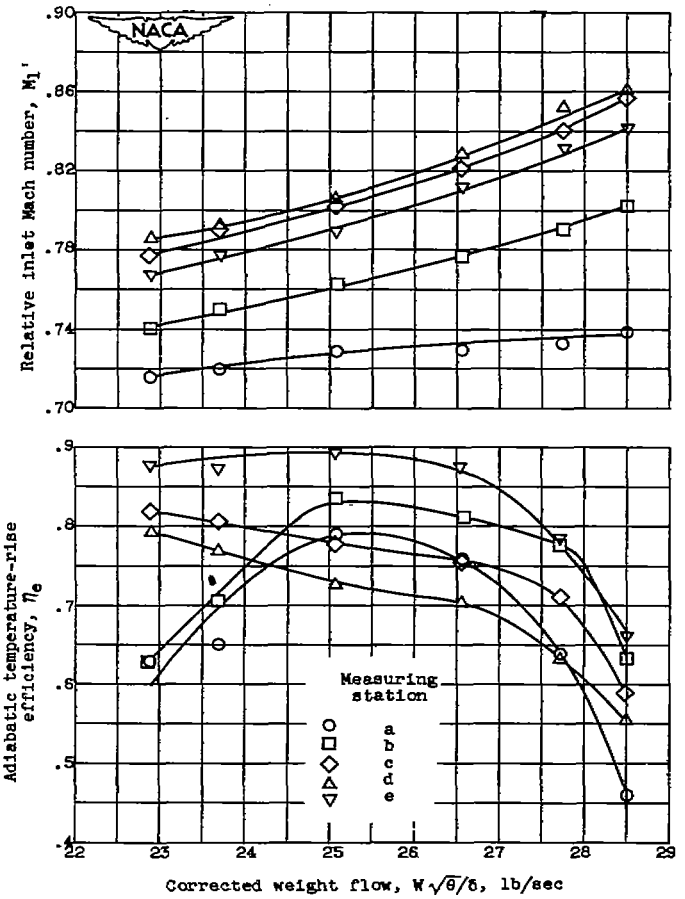

(a) Tip speed U_t, 1104 feet per second.

Figure 11. - Blade element performance characteristics of high-camber rotor with modified guide vanes.

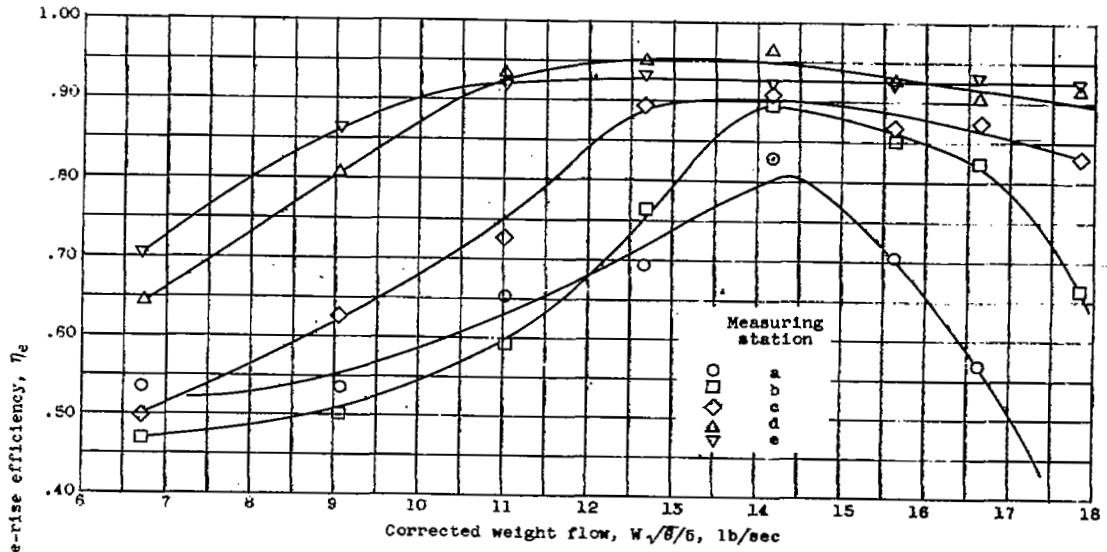

(b) Tip speed U_t, 552 feet per second.

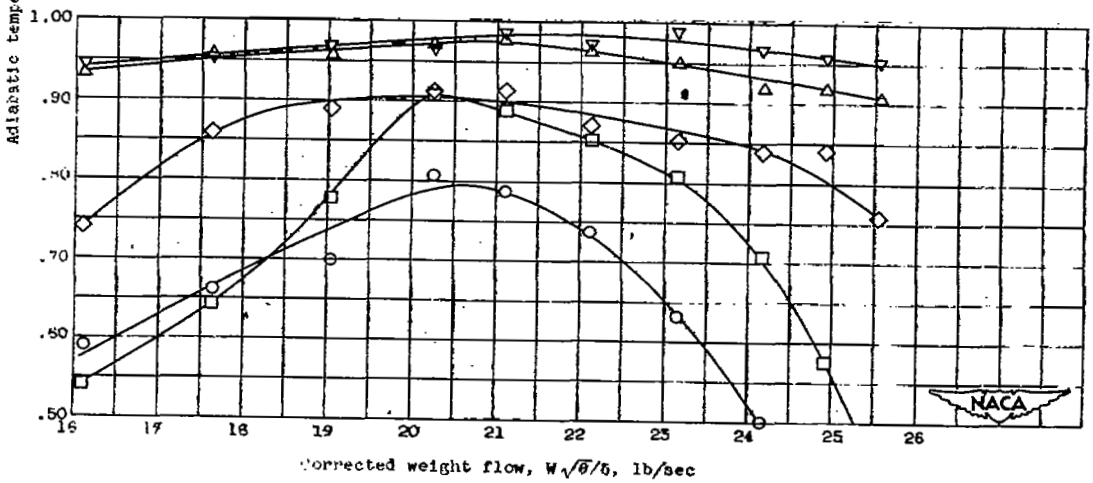

(c) Tip speed U_t, 828 feet per second.

Figure 11. - Concluded. Blade-element performance characteristics of high-camber rotor with modified guide vanes.

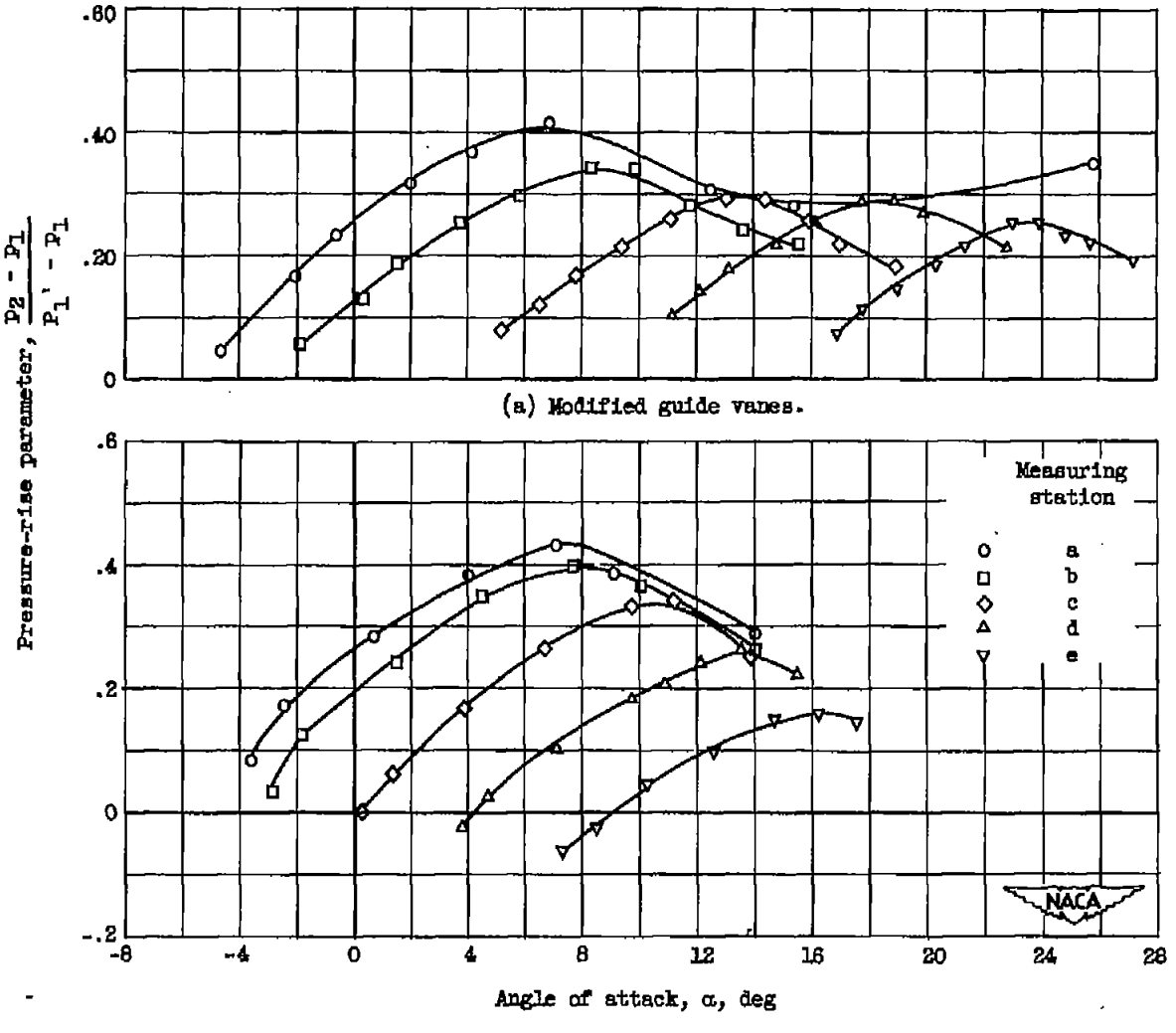

Figure 12. - Static-pressure-rise characteristics for original and modified stages. Tip speed U_t, 828 feet per second.

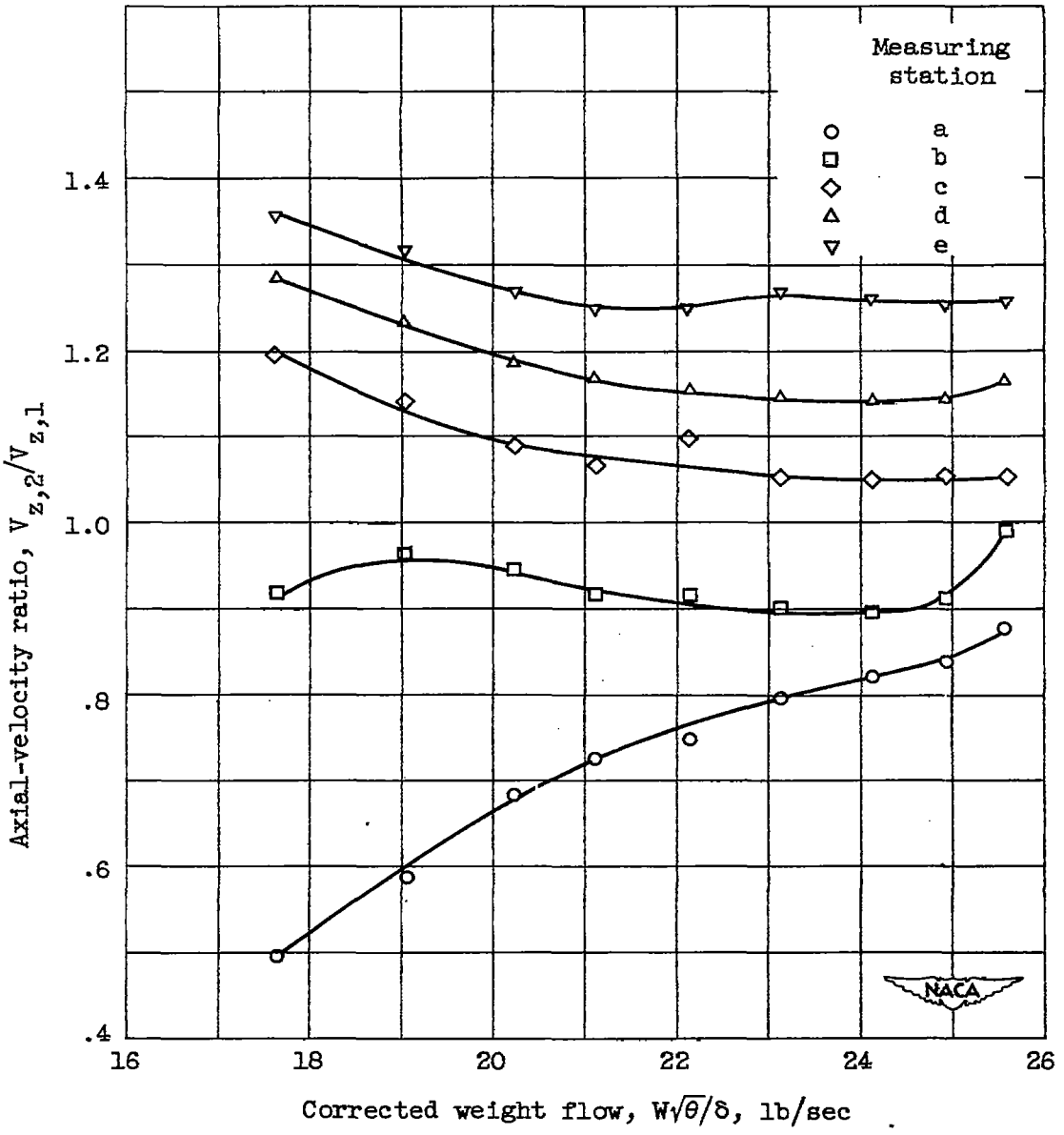

Figure 13. - Axial-velocity ratios for the high-camber rotor with modified guide vanes. Tip speed U_t, 828 feet per second.

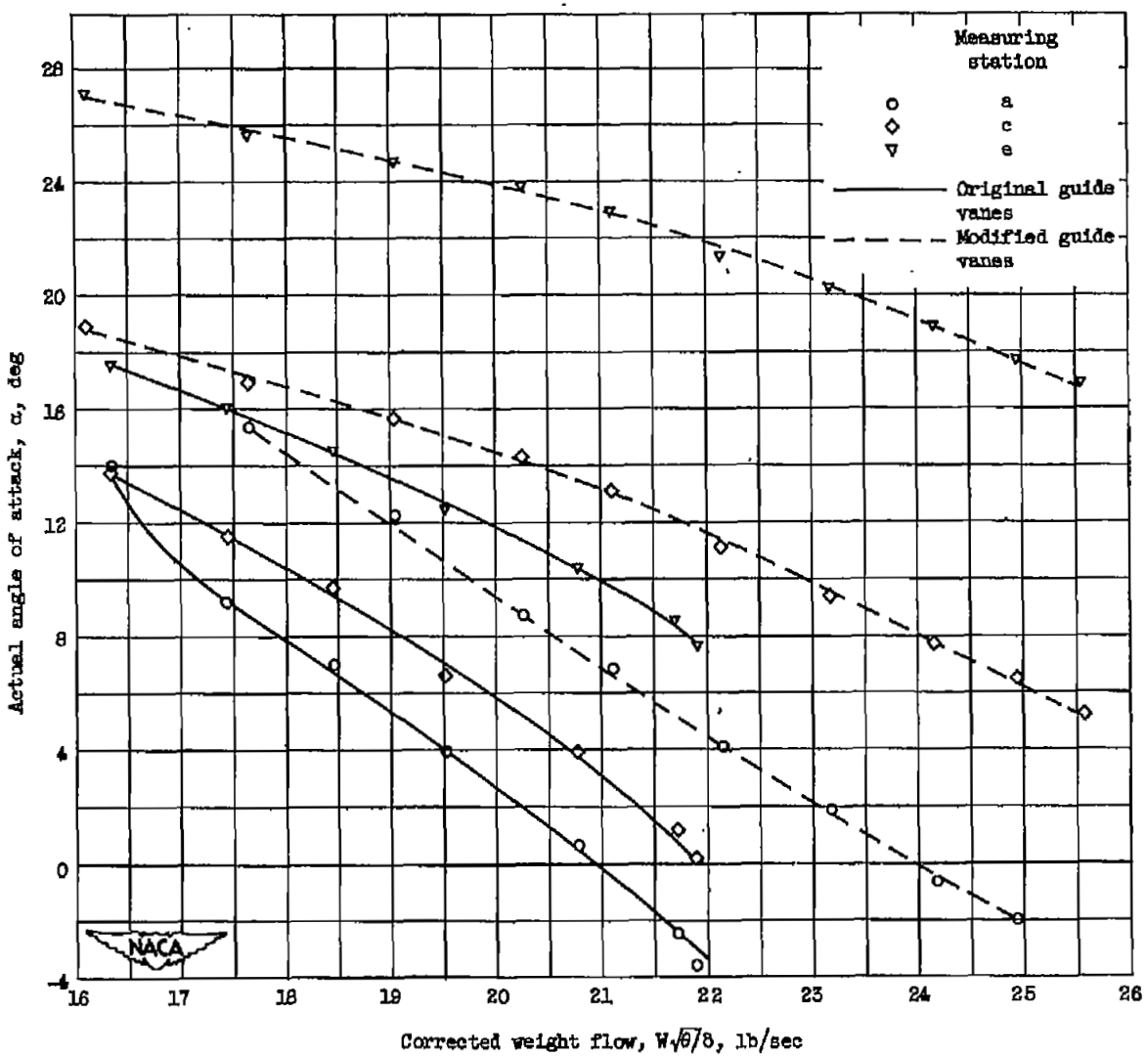

Figure 14. - Variation of angles of attack with corrected weight flow for original and modified stages. Tip speed U_t, 828 feet per second.

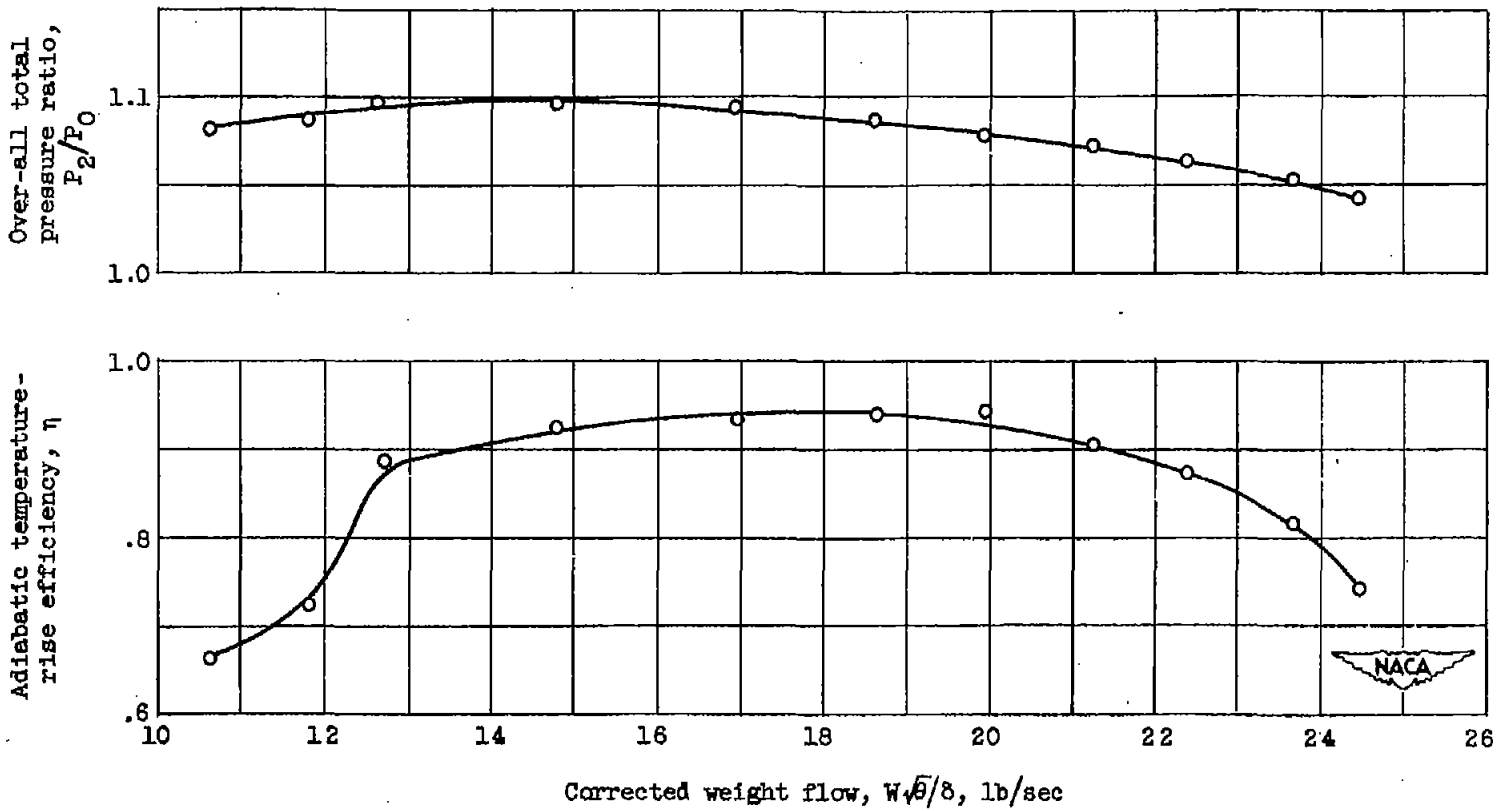

Figure 15. - Over-all performance of high-camber rotor without guide vanes. Tip speed U_t, 546 feet per second.

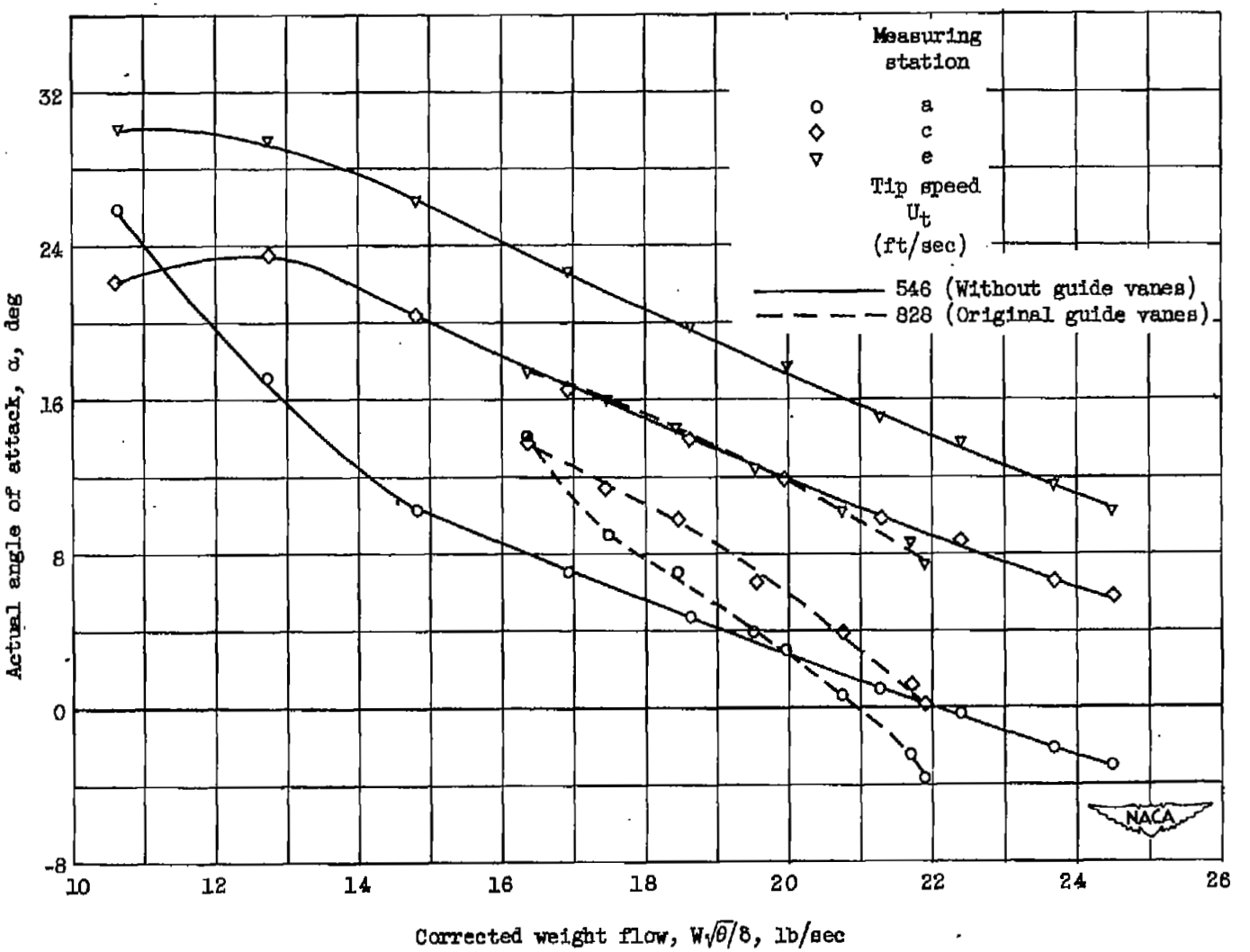

Figure 16. - Variation of actual angle of attack with corrected weight flow for high-camber rotor with original guide vanes and without guide vanes.

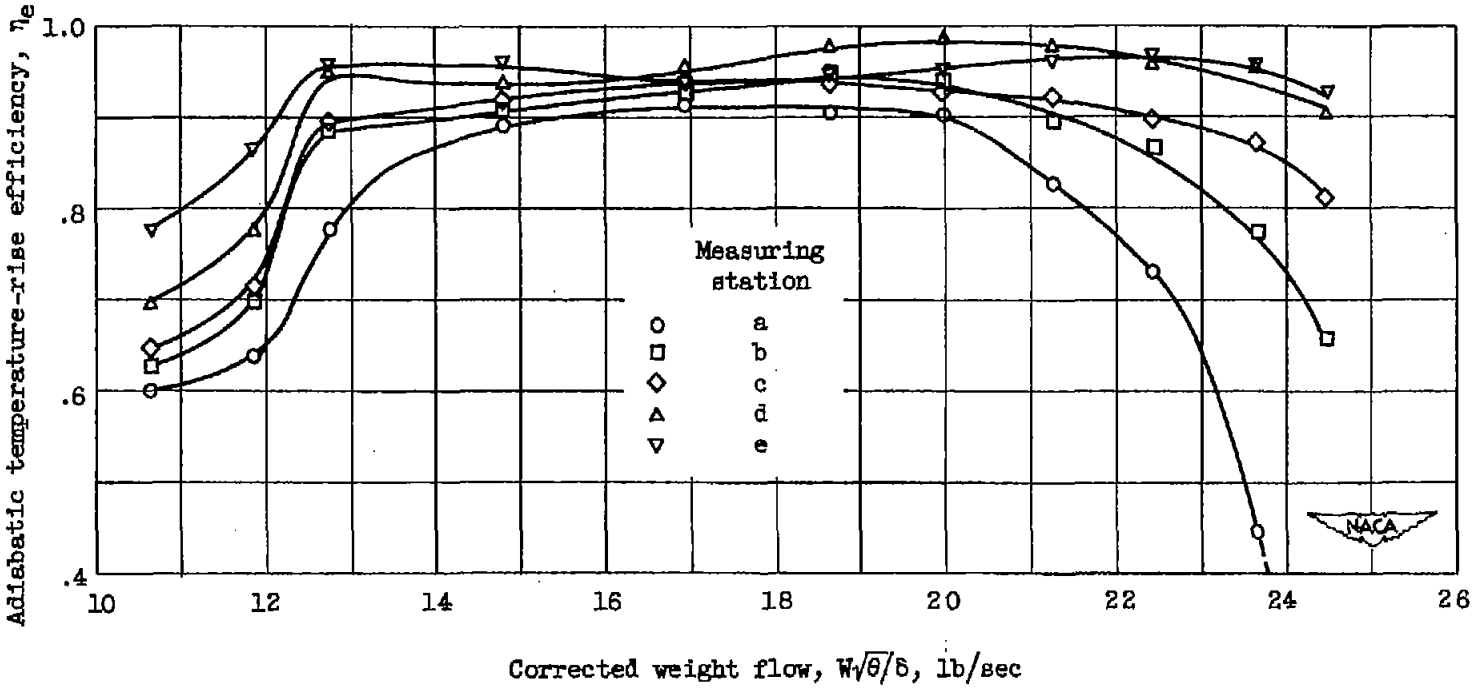

Figure 17. - Blade-element efficiency characteristics for high-camber rotor without guide vanes. Tip speed U_t, 546 feet per second.

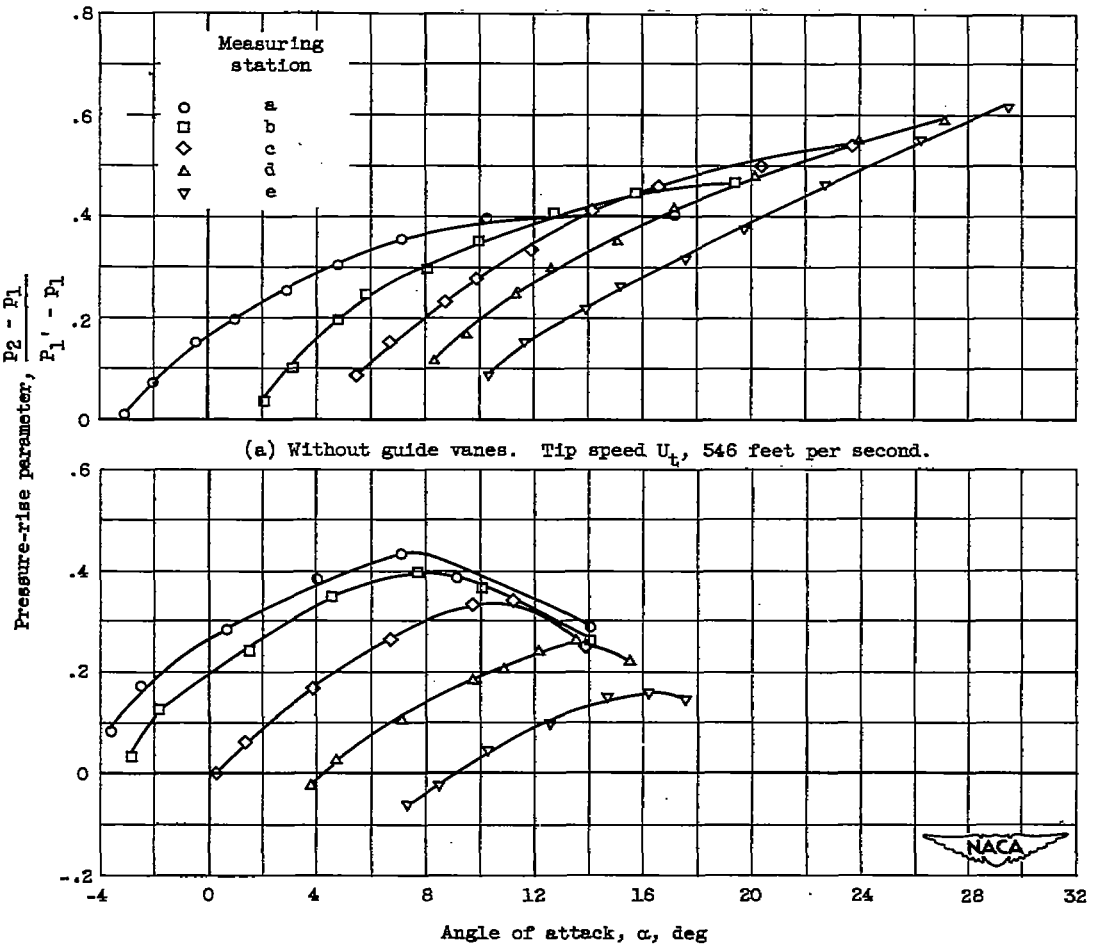

(a) Without guide vanes. Tip speed U_t, 546 feet per second.

(b) Original guide vanes. Tip speed U_t, 828 feet per second.

Figure 18. - Variation of pressure-rise parameter with angle of attack for high-camber rotor.

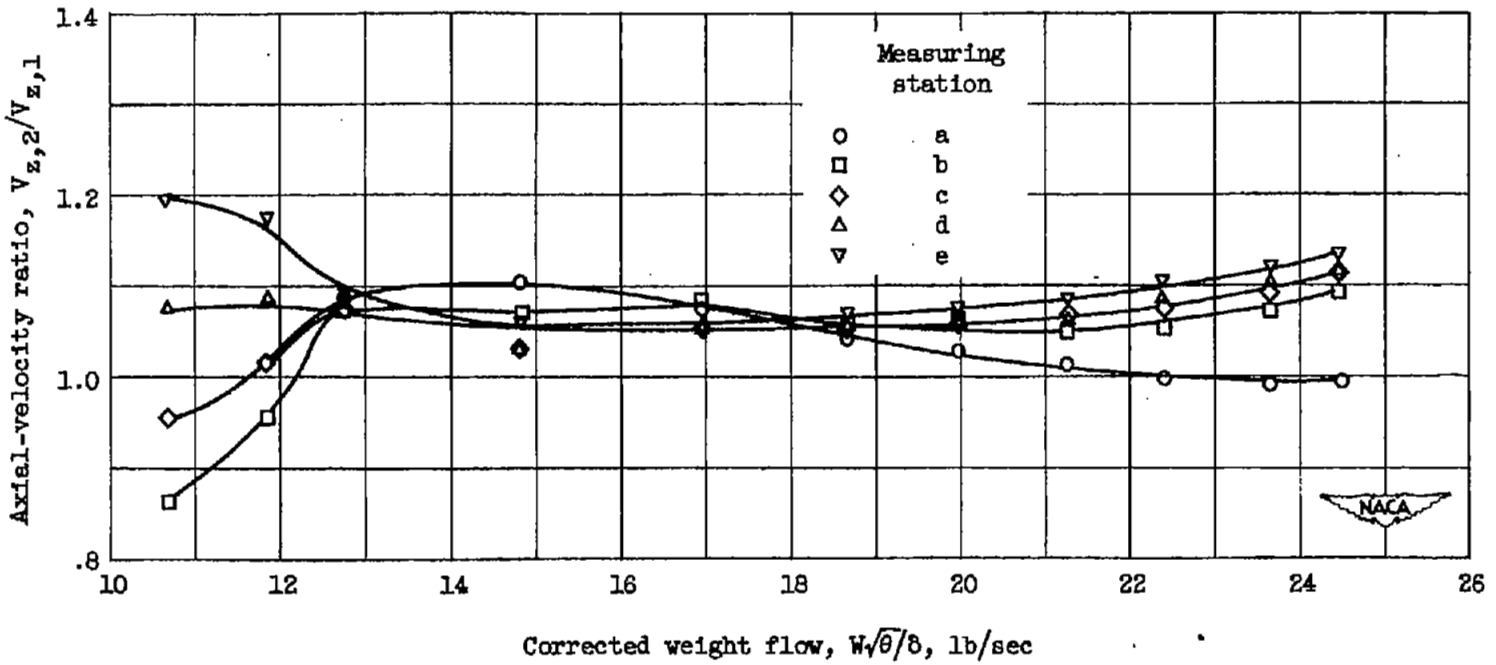

Figure 19. - Variation of axial-velocity ratio with corrected weight flow for high-camber rotor without guide vanes. Tip speed U_t, 546 feet per second.

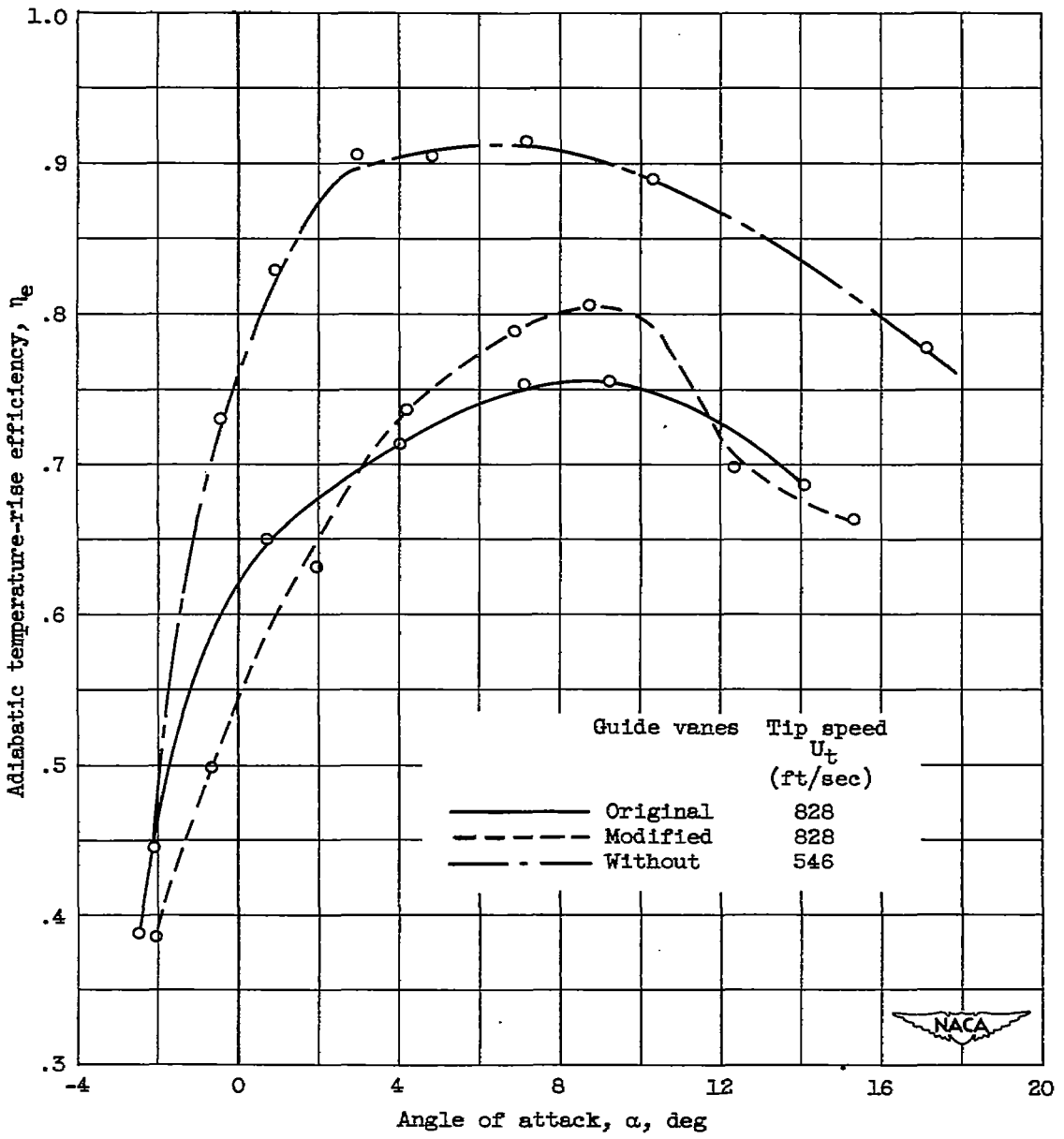

Figure 20. - Variation of adiabatic temperature-rise efficiency with actual angle of attack at measuring station a for high-camber rotor.

[redacted]

[redacted]